University of South-Eastern Norway

Faculty of Technology, Natural Sciences and Maritime Sciences

Master's Thesis
Study programme: Master of Environmental Science
Spring 2020

Konstanse Skøyen

The surface albedo of three lichen species (*Flavocetraria nivalis, Cladonia stellaris, Cetraria islandica*) and crowberry (*Empetrum nigrum*), and the influence of zenith angle, clouds and aspect

University of South-Eastern Norway
Faculty of Faculty of Technology, Natural Sciences and Maritime Sciences
Department of Natural Sciences and Environmental Health
PO Box 235
NO-3603 Kongsberg, Norway

http://www.usn.no

This thesis is worth 60 study points

Abstract

The surface albedo of vegetated surfaces can influence the climate through the fraction of the solar radiation that is reflected back to the atmosphere. In this study, I have measured the surface albedo of three lichen species *Flavocetraria nivalis, Cladonia stellaris*, and *Cetraria islandica*, and crowberry, *Empetrum nigrum*, with increasing cover in idealized field experiments performed in Bø, South-Eastern Norway, in April to June 2019. In addition, the impact of environmental factors that affect the reflection of solar radiation was studied. These factors include the solar zenith angle, aspect and cloud cover for explaining the variation in the surface albedo.

The results show that the surface albedo differs between species of different colors. The surface albedo decreases respectively for the different surfaces of *C. stellaris* (0.36), *F. nivalis* (0.34), 25 % *E. nigrum* (0.29), 50 % *E. nigrum* (0.23), 75 % *E. nigrum* (0.18), 100 % *E. nigrum* (0.15) and *C. islandica* (0.15). The surface albedo can differ within and between growth forms, and the *C. islandica* has similar surface albedo as total coverage of *E. nigrum*. With decreasing coverage of *C. stellaris* and increasing coverage of *E. nigrum*, the reflection of solar radiation decreases.

The surface albedo is also influenced by environmental factors. Clouds can lower the incoming solar radiation and show most effect on the albedo. With increasing cloud cover the influence of zenith angle and aspect can be lowered, where less radiation reaches the ground. Under cloudless conditions a north-facing slope receives less radiation than a south-facing slope. With increased cloudiness there is a smaller difference between these slopes.

A change in the surface albedo can influence the energy budget at the ground. Vegetation in alpine areas are changing. As a response to climate change, shrubs are expanding at the expense of lichens distribution where warmer climate conditions are more favorable for shrubs. For more accurate projections for the future climate, the influence of species on the surface albedo is important to understand.

Keyword: Surface albedo, field experiments, Southern Norway, fruticose lichens, evergreen shrub.

Table of content

Acknowledgments

I would like to thank my supervisors, Steffanie Reinhardt and Hans Renssen, and Peter Aartsma for letting me be a part of the surface albedo project at the University of Southeast-Norway. Many thanks to my friends for help and support along the way. I will especially thank Mie Prik Arnberg for statistical guidance and input during the process. I would also thank Frode Bergan for making the board for the surfaces, and other handy help. Also, I would like to thank Martin Hagen Ring, Jessica Kessler, again Mie Prik Arnberg, Ann-Cecilie Henriksen, and Monika Szaynok for helping me with transportation and sampling of lichens in the field. I would also like to thank the janitors at the school for help. I would like to thank Ann-Cecile Henriksen and Inga-Britt Morken for proofreading my thesis and much helpful inputs. Lastly, I would like to thank the academic writing center at the University of Southeast-Norway for proofreading.

Nittedal, January 2020

Konstanse Skøyen

1. Introduction

Alpine and arctic environments have been particularly affected by climate warming since the mid eighteenth century (IPCC, 2013). Fennoscandia is no exception, with a temperature increase of 0.5 °C per decade (1976 – 2014), and with future projections of further warming (Hanssen-Bauer et al., 2015). Vegetation is responding to the increased temperatures with upward migration of the treeline (Kullman, 2002; de Wit et al., 2014), expansion of shrubs (Sturm et al., 2001; Chapin III et al., 2005; Tape et al., 2006; Cannone et al., 2007), and change in species composition (Wilson and Nilsson, 2009; Michelsen et al., 2011). Increased vegetation greening has been detected on the Northern Hemisphere (Xu et al., 2013) and in alpine areas (Carlson et al., 2017), with an upward shift of plants and an increased species richness on mountain summits (Klanderud and Birks, 2003; Walther et al., 2005; Odland et al., 2010; Felde et al., 2012; Steinbauer et al., 2018). In response to climate change, vegetation can continue changing at different spatial and temporal scales (Pearson et al., 2013; de Wit et al., 2014). Lichens are, for instance, one growth form that can be negatively affected by changing climatic conditions.

In Scandinavia, mat-forming lichens are an important component of the alpine vegetation, contribute to a large part of the biomass (Porada et al., 2016), covering approximately 8 % of Norway (Bryn et al., 2018). Fruticose lichens are most common in the continental parts of Fennoscandia (Moen, 1999) and in boreal and arctic ecosystems (Ahti and Oksanen, 1990). In those areas, lichen biomass is also influenced by reindeer (*Rangifer tarandus*) grazing, as lichens are important forage during winter (Den Herder et al., 2003; Ims Vistnes and Nellemann, 2008; Tømmervik et al., 2009; Odland et al., 2014).

In alpine areas, the distribution of lichens are associated with a thin or lacking snow cover (Bruun et al., 2006; Löffler, 2007; Odland and Munkejord, 2008; Bidussi et al., 2016), and high lichen cover is negatively correlated with cover of vascular plants in alpine (Bruun et al., 2006; Odland et al., 2015) and arctic areas (Cornelissen et al., 2001). Environments with low soil temperatures in combination with other harsh climatic conditions, such as permafrost, can facilitate lichen abundance and reduce the cover of taller vascular plants (Kershaw, 1978; Sundstøl and Odland, 2017).

As a result of climate change, lichens can respond negatively in abundance with increased competition from shrubs. This effect on lichens is found in Scandinavia with increased cover in the crowberry (*Empetrum nigrum*) (Vanneste et al., 2017; Vuorinen et al., 2017; Maliniemi et al., 2018). The negative effect on lichens is due to the shrubs shading and litter accumulation (Jonasson, 1992; Press et al., 1998; Cornelissen et al., 2001; Klanderud and Birks, 2003; Jagerbrand et al., 2006; Dawes et al., 2011, Lang et al., 2012). Lichens can also reduce their coverage in experiments with induced warming while vascular plants increase their coverage at the expense of lichens (Walker et al., 2006; Klanderud, 2008; Dawes et al., 2011; Elmendorf et al., 2012). It is likely that these changes will continue.

Vegetation is not only affected by climate, and can also influence the climate in many ways, for instance by its surface albedo. The surface albedo is the ratio between reflected and incoming shortwave solar radiation at the ground, and is presented as a number between 0 to 1 (Oke, 1987)(Equation 1.1),

$$\alpha = \frac{K_{out}}{K_{in}} \qquad \text{Eq. 1.1}$$

where α is the surface albedo, K_{out} is the reflected shortwave radiation, and K_{in} is the incoming shortwave radiation from the sun (Oke, 1987). The amount of solar radiation that is reflected by the ground depends on the actual surface. For instance, *Cladonia stellaris* dominated heaths have higher surface albedo and lower soil temperatures compared to surfaces of growth forms such as bryophytes (Stoy et al., 2012). Solar radiation that reaches the ground is transformed into thermal energy that warms the Earth's surface (Oke, 1987). The albedo of vegetation surfaces can vary substantially, and vegetation change can lead to increased surface temperature at local and regional levels (Pearson et al., 2013; Fraser et al., 2014; Duveiller et al., 2018). Lichens have the ability to influence the local climate and have a cooling effect on the environment. This effect by mat-forming lichens is found at a larger scale on the Northern Hemisphere (Porada et al., 2016). Further expansion of shrubs and decrease in light lichens can reduce the surface albedo, give regional warming, and facilitate further global climate warming (Wookey et al., 2009; Myers-Smith et al., 2011). This can have a negative impact on alpine vegetation and especially the lichens distribution (Fraser et al., 2014).

The reflection of shortwave radiation from vegetated surfaces can differ between growth forms, such as lichens and shrubs. As an example, lichen-dominated vegetation can have a surface albedo of 0.19 compared to 0.15 of deciduous shrubs (Williamson et al., 2016). This is also found in studies on alpine and arctic vegetation where the surface albedo of vegetation types containing light lichens is higher than for vegetation types with reduced or no lichen cover (Beringer et al., 2005; Bernier et al., 2011; Tømmervik et al., 2012; Cohen et al., 2013). In these studies, the effect of lichens on the surface albedo depends on the coverage and height of the shrubs and trampling and grazing on vascular plants and lichens.

Despite the potential decrease of lichen coverage that can result in lower albedo at the ground, there is a lack of species-specific studies on lichens. The surface albedo within and between growth forms can differ, as for instance lichens differ in terms of color and structural building. Some lichens are known for their light colors and high albedo such as *Cladonia* spp., and their surface albedos have been addressed (Cornelissen et al., 2007; Joly et al., 2009; Odland et al., 2018).

The mat-forming lichens with a light color show a higher reflection of solar radiation than most other surfaces. Field measurements of the albedo of light lichens have resulted in values of 0.26 compared to 0.12 for black spruce forest (Petzold and Rencz, 1975). Light lichens in woodland can have an albedo of 0.29 (Kershaw, 1978). In experiments with radiometers higher values have been revealed on *C. stellaria* with 0.31, and 0.20 for lingonberries (*Vaccinium vitis-idaea*) (Peltoniemi et al., 2010). Another experiment found a mean surface albedo of 0.33 for *Cladonia* spp. (Heim and Lundholm, 2013). These studies show that light lichens have the ability to reflect more solar radiation than other types of vegetation. Despite these differences, the lichens ability to affect climate is poorly understood.

The surface albedo in small- and large-scale studies do differ, and the albedos of vegetation types are lower at larger scales than for target specific measures (Oke, 1987). One reason why surface albedo is lower at larger scale is due to the heterogeneity in the vegetation. Surface albedo studies with satellite images can use few vegetation categories and lichens are included in categories that also contain other growth forms. The precision of the surface albedo from satellite images depends on the image resolution where lichen tundra can be difficult to distinguish from for example shrubby tundra (Virtanen and Ek, 2014). In addition, field measurements can be influenced by the surrounding vegetation and give less accurate albedo values of the vegetation surface. These drawbacks make it more difficult to determine the effect of species-specific contribution on the surface albedo.

A generalization of the surface albedo of alpine vegetation is complex to determine. For instance, the reflection of solar radiation might not differ between vegetation types despite being visually different (Blok et al., 2011). In addition, Juszak et al. (2014) showed that simulated increase in Dwarf birch (*Betula nana*) density and biomass did not change the amount of reflection of solar radiation from the shrub surfaces. Other studies have found that a transition from lichen- to shrub- and forest vegetation can lead to reduced reflection of radiation with increase of shrub- and tree biomass and density (Thompson et al., 2004; Williamson et al., 2016).

Still, the surface albedo of lichens has received little attention despite that they are an important component in the alpine vegetation. Most studies on surface albedo have focused on vascular plants, and especially on shrubs where lichens are excluded or part of few vegetation classes in combination with vascular plants (Eugster et al., 2000; Loranty et al., 2011; Bonfils et al., 2012). In vegetation studies, lichens are often excluded or lumped together with bryophytes as cryptograms (i.e. Graglia et al., 2001; Cornelissen et al., 2007; Porada et al., 2016; Vanneste et al., 2017). This makes it difficult to assess the importance of lichens in alpine landscapes and their contribution to the ground radiation budget.

A change in the vegetations composition can influence the climate at the ground with increased absorption of radiation. "Shrubification", the expansion of woody shrubs (Myers-Smith et al., 2011), is predicted to continue at different scales in alpine (Mod and Luoto, 2016) and northern areas (Swann et al., 2010; Pearson et al., 2013; de Wit et al., 2014; Rydsaa et al., 2017). Such a vegetation change can eventually increase the soil temperature and reduce areas with permafrost that generate a higher root depth and facilitate shrub growth (Wookey et al., 2009; Lawrence and Swenson, 2011). The shrubification can give new surface albedo dynamics, and eventually impact the radiation budget at the ground that is defined as (Oke, 1987) (Equation 1.2),

$$Q^{*} = (K_{in} - K_{out}) + (L_{in} - L_{out}) \quad \text{Eq. 1.2}$$

where $Q*$ is the net radiation, K_{in} is the incoming shortwave solar radiation, K_{out} is the reflected shortwave radiation, L_{in} is the incoming longwave radiation from the atmosphere, and L_{out} is the outgoing terrestrial longwave radiation, measured in W/m^2 (Oke, 1987). The surface albedo is therefore an essential part of the net shortwave solar radiation and thus the radiation budget at the ground.

The proportion of incoming and reflected shortwave radiation are influenced by environmental factors. These factors are compound, and some of the most influential are time of the year and day, the solar zenith angle, topography and aspect, clouds and other atmospheric components such as aerosols (Oke, 1987; Ramanathan et al., 1989; Oliphant et al., 2003). In addition, for the surface albedo the radiative properties and structure of the surface is also important (Oke, 1987). These factors can all explain variations in the albedo for a surface.

The changes in incident solar radiation is dependent on the season, and especially at higher latitudes there are great differences in incoming solar radiation between summer and winter. During the growing season, the amount of incoming solar radiation increases at the higher latitudes (Oke, 1987; Ohmura, 1982; Sturm et al., 2005). Diurnally the surface albedo varies due to incident solar radiation, where morning and evening albedos are higher than midday (Oke, 1987). On cloudless days, the surface albedo decreases with decreasing zenith angle (Pirazzini, 2004). The diurnal variation in albedo on the radiation budget is small, because the highest albedos occur at times with low radiation input (Oke, 1987).

The alpine landscape is characterized by large variation in topography, and therefore the surface albedo will have large variations between slopes and aspect in the terrain. The orientation of a surface influences the amount of incident radiation it receives. The incident sunlight therefore varies spatially depending on the topography and the angle of incoming radiation (Oke, 1987).

In summer at high latitudes, north-facing slopes receive solar radiation in the morning and evening, and south-facing slopes receives directly solar radiation when the position of the sun is higher (Oke, 1987; Bennie et al., 2008). The topographical variations thus lead to differences in the energy budget at local levels and the highly changing microclimates in alpine areas (Oke, 1987; Bennie et al., 2008; Opedal et al., 2015). This can be reflected in the distribution of snow cover and vegetation (Oke, 1987; Cherubini et al., 2017). For instance, south-facing slopes can have a higher treeline that receives more radiation than north-facing slopes (Odland, 1996).

The fraction of incoming solar radiation that reaches a surface can be heavily influenced by clouds (Ramanathan et al., 1989). Solar radiation that passes through the atmosphere encounters atmospheric components such as clouds, water vapor, salt crystals, dust particles and different gasses (Moene & Dam, 2013). The absorption of shortwave radiation in the atmosphere depends thus on the atmospheric components, where clouds are the most effective reflector and scatter of solar radiation (Oke, 1987; Kim and Ramanathan, 2008).

To get a better understanding of lichens and shrubs surface albedo, a species-specific study is essential for more accurate projections for the surface albedo of alpine vegetation. In addition, it is important to consider how environmental factors can affect the albedo of lichen surfaces. In this project, I have performed a set of idealized experiments with the aim to:

1) Measure the surface albedo of three lichen species *Flavocetraria nivalis, C. stellaris*, and *Cetraria islandica*, and one evergreen low growing shrub, *E. nigrum*.
2) Study the impact of the solar zenith angle, aspect, and cloud cover on the surface albedo.

2. Methods

2.1 Study species

In this study, I measured the surface albedo of three lichens species, *C. stellaris*, *F. nivalis* and *C. islandica*, including increasing cover of the evergreen and woody shrub *E. nigrum*. All three study species are mat-forming and common in alpine vegetation of Fennoscandia. However, their distribution differs, and are important components in different vegetation types.

F. nivalis is common in the Northern Hemisphere, in arctic and alpine areas (Ahti & Oksanen, 1990; Walker, 2006), and is also found in Antarctica (Bjerke, 2004). In alpine areas it grows on exposed ridges with *Alectoria ochroleuca* where snow cover is shallow or absent and has a decrease in coverage with increasing snow cover (Löffler, 2007; Bidussi et al., 2016). Other species with a wider range of different snow cover also grow with *F. nivalis*, such as dwarf birch (*B. nana)* (Ahti & Oksanen, 1990). It can also grow in communities with *C. stellaris* on upper slopes or ridges (Oksanen et al., 1995; Löffler, 2007). It is characterized as a light-colored lichen species with thick and curly branches.

C. stellaris is common in alpine and arctic areas and is dominant in the northern boreal forest (Ahti and Oksanen, 1990; Kershaw, 1978; Walker et al., 2005). It is an important reindeer forage during winter along with other species (*Cladonia* spp.) (Gaare et al., 2005; Joly et al, 2009). It dominates on the upper slope of ridges with more snow cover than *F. nivalis* with about 10-30 cm depth of snow (Löffler, 2007). *C. stellaris* is abundant in old stages of boreal forest, however it can also be among the first colonizers (Ahti and Oksanen, 1990; Kershaw, 1978). It can also grow in dwarf birch *(B. nana)* and *E. nigrum* vegetation (Oksanen, 1995). The lichen is a light-colored species with thin branches and cloud-like shape.

C. islandica grows in alpine, arctic and boreal forest (Ahti & Oksanen, 1990), and is also found in central Europe (Hauck, 2009). It can grow in moist habitats and can be dominant in snow beds (Odland et al., 2014), but can also be abundant in drier environments (Ahti & Oksanen, 1990). *C. islandica* can be common in communities with an get early snow cover, and is less wind resistant than *C. stellaris* (Ahti & Oksanen, 1990). It is associated with higher soil temperatures than the lichens growing on exposed ridges (Sundstøl et al., 2018). It can also grow in communities with dwarf birch *(B. nana)*, *E. nigrum* and *C. stellaris* (Oksanen et al., 1995). *C. islandica* is a dark brown lichen species with thick branches, with a lighter color on the underside.

The evergreen shrub *E. nigrum* is common in the same environments as the three lichens species. It is associated with thin snow cover and can be dominant in the alpine landscape (Tybirk et al., 2000; Odland and Munkejord, 2008). It is also considered as a keystone species in northern ecosystems (Väisänen et al., 2013; Bienau et al., 2015). It has dark green needlelike leaves, and brown branches.

2.2 Experimental design

The surface albedo was measured on a flat lawn on the campus of the University of Southeast-Norway in Bø (59°24'47"N, 9°04'10"E), in Telemark county, from April to June 2019. The three lichen species were sampled in two alpine areas, Imingfjell and Båttjønndalen. Sampling was done in August and September 2018, and March 2019. *E. nigrum* was sampled between May – June 2019 in Bø municipality one day before each measurement to maintain freshness.

The lichen species were sampled in small cushions, as homogenous and compact as possible. The individual lichen species were inserted into perforated boxes to prevent rotting. Then, other lichen specimens and organic matter was removed. In natural environments, other species of lichens, bryophytes and vascular plants grow in between the mat-forming lichen species.

As mentioned before, several environmental factors can influence the amount of solar radiation (solar zenith angle, clouds, aspect, etc.), and these factors were considered for each of the measurements. The measurements started and ended on a horizontal surface each day, and the cloud cover was observed and classified for each measurement of the surface albedo. The measurements were paired, where two species were measured at the same time (Table 1).

Zenith angle

The solar zenith angle influences the surface albedo by the amount of incoming solar radiation that hits a surface. It is the angle between the direction to the sun and the normal to the surface (Coakley, 2003). Measurements in this experiment were done at specific zenith angles and specific aspects throughout the study period. All aspect categories besides horizontal surface at noon (HSN) have constant zenith angle, where HSN has a decreasing zenith angle through the whole study period (Figure A5; Table 1; Table A5).

In the Northern Hemisphere, the seasonal variation in zenith angle is considerable. At the latitude of Bø in Telemark (i.e. 59°N), the sun angle during winter is too low and the proportion of shortwave solar radiation that reaches a surface is heavily reduced. Therefore, this experiment was run when the zenith angle was below 60° in April during daylight when the amount of solar radiation is higher. The zenith angle was controlled by using a scheme with specific zenith angles through the whole study period. The zenith angles were decided before running the experiment. Measurements started and ended at the same zenith angle each day, with increase in time between intervals from the start to the end of the study period to match the specific zenith angles. Therefore, the different surface albedo measurements using the specific zenith angles from day to day measurements are directly comparable.

Aspect

In this study, the aspect was categorized in three ways; horizontal surface for all species, and 10° north- and south-facing for *F. nivalis* and *C. stellaris* (Table 1). In the Northern Hemisphere, south facing and horizontal surfaces show symmetrical energy receipt on midday (Oke, 1987). A north-facing surface will be influenced by shading and receive less solar radiation than a south-facing surface.

The *F. nivalis* was measured during the whole study period and was paired with one of the other species. The study started with additionally measuring *C. stellaris*, then *C. islandica*, then increasing cover of *E. nigrum* from 25 %, 50 %, 75 %, and finally 100 % coverage. The first pair of surfaces had seven different interval of surface albedo measurements for one day. The next pairs of surfaces had three intervals with only horizontal surfaces. The different aspect categories also match specific zenith angles. The sampling regime with aspect categories is presented in Table 1 and Table A5.

Cloud cover

Cloud cover observations were categorized for each paired measurement of the surface albedo (Table A5). The cloud cover was estimated by observations, and each interval got one individual cloud cover category. The cloud cover was categorized using a meteorological scale from 0 to 8 in okta units, where 0 represent no cloud cover, and 8 represent full cloud cover. The cloud cover was observed by one person, to reduce bias on the cloud cover observations.

Clouds can be very effective in reflecting and scattering solar radiation (Oke, 1987). This can change over short time periods and can be seen as fluctuations in measurements of shortwave radiation due to absorption and reflection by clouds (Oke, 1987). On a clear day, surface albedo measurements are therefore displaying a smooth curve. The fluctuations in cloud cover is not accounted for in the observations as the cloud cover is registered only one time during one surface albedo interval. The influence of clouds has also been measured by calculation of cloud factor for each surface albedo interval (see data analysis).

The cloud cover observations did not measure all atmospheric particles causing scatter or reflection of radiation, such as the cloud factor. Also, cloud cover categories can be less precise as cloud cover is only observed once during each measurement. The cloud cover can change rapidly, and this is not considered in the cloud cover observations. In addition, observed clouds might not shade for the incoming sunlight and thus do not reduce the amount of incoming radiation.

Radiometer

A CNR 4 net radiometer (Kipp & Zonen, Delft, the Netherlands) measured the incoming and reflected shortwave solar radiation, between 300 to 2800 nm, for each surface. Two radiometers were used in this experiment. The radiometer consists of a pyranometer pair, one facing upwards, the other facing downwards. The output units is expressed in Watts per square meter (W/m^2). The up- and downward facing pyranometers measure the energy that is received from the whole hemisphere with a 150° field view (Kipp & Zonen, 2014). The measurement radius of the radiometer is approximately 75 cm when the radiometer is placed at a height of 20 cm. When the radiometer is lower than 150 cm the instrument can shade the surface. The radiometer should be installed horizontal over the surface (Kipp & Zonen, 2014).

The incoming- and reflected shortwave radiation hitting the pyranometers was logged. The datalogger logs data every five seconds and gives an average for every one minute. One interval in the experiment was set to 30 minutes. The surface albedo was calculated as an average of 30 minutes for surface albedo analysis.

The surface albedo should be a number between 0 and 1 and checking this can be a tool for quality assurance of the measurements (Kipp & Zonen, 2014). It is also important to check the curve of the shortwave radiation from the pyranometers. Under perfect conditions, measurements from the pyranometers of solar radiation will have a cosine response curve (Kipp & Zonen, 2014).

It was not recommended by the manufacturer to do measurements when the solar zenith angle was higher than 80°, the sun angle is too low and the proportion of radiation that reaches a surface will be heavily reduced, and causes unreliable results (Kipp & Zonen, 2014). Errors of surface albedo measurements can also occur when there is precipitation. Therefore, in this experiment, measurements started with a solar zenith angle below 60° and without precipitation.

Experimental setup

The species in this study are represented by seven individual surfaces; three lichens and four different covers of *E. nigrum* combined with *C. stellaris*. One species was covering one experimental surface. Two experimental surfaces, or species, were measured at the same time through the whole study period. During the whole study period the surface albedo was measured for *F. nivalis* paired with one of the other six surfaces; starting with 1) *C. stellaris*, 2) *C. islandica*, 3) 25 % cover of *E. nigrum*, 4) 50 % cover of *E. nigrum*, 5) 75 % cover of *E. nigrum*, and finally 6) 100 % *E. nigrum* (Table 1). Most measurements were therefore conducted for *F. nivalis* compared to all the other species (Table 1). The lichens were stored dry, cold and dark, to prevent damage or color change due to mold and sunlight.

The three different lichen species were each covering one individual surface, consisting of a circular flat wooden board with a diameter of 1.75 m. The edge of the board was fitted with vertical mesh of 10 cm to keep the lichens in place. To cover the surface of 1.8 m^2 the amount of lichen was dependent on the lichen species, and approximately 1.8-2.0 m^2 was needed for tightly packing one surface depending on the species. The lichens were packed as tight as possible to create a cover of approximately 100 %, and to prevent reflection of solar radiation from the underlying board surface. One surface was representing one lichen species, resembling their natural appearance. The lichen surfaces were watered to prevent open cracks on the surfaces. Wind and sun dry up the lichens during a whole day of measurements.

After running the surface albedo measurements on *C. stellaris* and *C. islandica*, measurements on *E. nigrum* started with increasing cover on top of *C. stellaris*. The round *C. stellaris* surface was divided into parts of 25 %, 50 %, 75 % and 100 % cover of *E. nigrum* (see picture for *E. nigrum* coverage). The *E. nigrum* branches were placed maintain a horizonal surface on top of the *C. stellaris*, starting with the lowest percentage cover of 25 %, and increasing the coverage after conducted enough surface albedo measurements at each cover.

The surfaces were placed away from disturbing elements, such as trees and buildings that could shade or reflect sunlight on to the experimental surfaces. The two paired surfaces were placed side by side at the same individual location every day.

The surfaces were leveled with a clinometer that measures the angle of a slope, to have either horizontal, 10° north- or south-facing surface to measure surface albedo at different aspects. One day of measurements on *C. stellaris* and *F. nivalis* were done at horizontal surface in the morning, north-facing surface at morning, south-facing surface at morning, horizontal surface at noon, north-facing surface at afternoon, south-facing surface at afternoon, and finally horizontal surface at afternoon. Only the first pair of surfaces, *C. stellaris* versus *F. nivalis,* was measured with north- and south-facing aspect. The *C. islandica* and all the covers of *E. nigrum*, were measured three times during one day with a horizontal surface (Table 1; Table A5).

Above each surface, a radiometer was placed following the manual from Kipp & Zonen (2014). The radiometer was placed 20 cm above each surface on a pole going through the board. The pole was positioned on the northern side of the board, and the radiometer was attached on a 65 cm arm facing south from the pole. This placement prevents shading from the pole and the arm from the radiometer on the surfaces.

The 20 cm height of the radiometer was resulting in a circular measurement surface of 1.5 m^2 from the pyranometers. To prevent disturbance on the surface albedo measurements a buffer zone of 15 cm was added on the edge of the board outside. The vegetation surrounding the experimental surfaces changed during the study period, starting with brown and low vegetation in April, and with taller green vegetation in June. Shading from the surrounding vegetation could decrease the incoming sunlight. However, by adding the buffer zone (15 cm) and by adjusting the height of the radiometer (20 cm), the potential error was accounted for. Hence, the measurement surface of the radiometer did only cover the lichen surface.

The pyranometers on the radiometer were in the center of the experimental surface. The pole stand was attached with bar stools to prevent it displacing due to wind during measurement intervals. The radiometer was leveled to stand perpendicular over the lichen surface. Height and displacement were adjusted between each interval. In addition, for each interval a picture was taken to document set-up and the cloud cover.

Each radiometer had its own compatible data logger, LOGBOX SE, Kipp & Zonen, Delft, the Netherlands. The radiometers with its data logger were switched between the two experimental surfaces to prevent bias of the radiometers. Incoming longwave radiation from both radiometers was plotted after each day of measurements. The data of the two radiometers did not show a difference in incoming longwave radiation and showed no difference between the radiometers. Also, surface albedo was plotted to check for eventual changes in surface albedo measurements.

Each surface albedo measurement had 30 minutes intervals with matching zenith angle through the study period, except for the noon measurements that had decreasing zenith angle from start to end of the measurement period. All days of measurements started and ended with the same zenith angle and aspect (Table 1; Table A5).

2.3 Data analysis

In the statistical analysis, only surface albedo measurements were included with solar zenith angle of more than 60°, and without precipitation. In total, there were 300 individual measurements.

For the statistical analysis, the aspect categories were merged and divided into four categories; 1) horizontal surface at morning and afternoon (HSMA), 2) horizontal surface at noon, 3) north-facing surfaces (NO) and 4) south-facing surface (SO).

The nine cloud cover categories were merged into three groups (group 1:0/1/2, group 2: 3/4/5, group 3: 6/7/8). These groups were used to calculate mean, standard deviation (SD) and minimum and maximum range for different subsets for the species.

Mean values were used for surface albedo and cloud factor (see below) for all surfaces, and mean, standard deviation (SD), and minimum and maximum range values were calculated. Different subsets for *C. stellaris* and *F. nivalis* were divided by the different aspect categories and for cloud cover categories.

The surface albedo was calculated from measurements of the pyranometers on the radiometer (Kipp & Zonen, 2014) (Equation 2.1),

$$\alpha = \frac{(E\ lower\ pyranometer)}{(E\ upper\ pyranometer)} \quad \text{Eq. 2.1}$$

where *E* is the ratio between voltage and a calibration constant for each of the lower and upper pyranometers (Kipp & Zonen, 2014). The ratio between the pyranometers also reflects the Equation 1.1 for the theoretical surface albedo, where the lower pyranometer represents the reflected shortwave radiation, and the upper pyranometer represents the incoming shortwave radiation. This gives a proportion of reflected radiation between 0 and 1. The structure and angle control the amount of penetration, radiation trapping, and shading within a vegetation surface (Oke 1987). For a generalization of the albedo for a surface it is therefore important that the surface is homogenous (Oke, 1987).

In the statistical analysis, an average of the 30 minutes intervals was used, with one interval being represented by one individual surface albedo value.

To analyze the influence of clouds, a cloud factor was calculated for each of the surface albedo intervals. Clouds can reduce the amount of incoming solar radiation that reaches a surface (Oke, 1987). The solar radiation that passes through the atmosphere encounters atmospheric components that have their own radiative properties when hit by the incoming shortwave solar radiation (Oke, 1987). About 50 % of the solar radiation does not reach the Earth – atmosphere system or is reflected by the atmosphere. Almost one half of the solar radiation is absorbed by the surface and transformed into thermal energy that warms the Earth's surface (Oke, 1987). In general, the atmosphere is not a good absorber of shortwave radiation and the absorption depends on the amount of clouds, atmospheric gasses and other aerosols (Oke, 1987; Li, 1998).

The incoming shortwave radiation varied seasonally and diurnally and is therefore included in the cloud factor calculation. The cloud factor was the proportion between incoming shortwave radiation ($K_{in,\ measured}$) measured at the surface and potential incoming shortwave radiation ($K_{in,\ potential}$) from the top of the atmosphere. Zero represents no influence of atmospheric properties, and one represents the influence of the atmospheric properties (Moene & van Dam, 2013).

To estimate the influence of clouds, the calculation of the potential incoming radiation (Equation 2.3) was used to calculate the cloud factor. Since the atmosphere can consist of different components that affect the amount of solar radiation that reaches a surface, the ratio between measured ($K_{in,\ measured}$) and potential ($K_{in,\ potential}$) incoming shortwave radiation was included. The cloud factor is calculated from Equation 2.2, see below,

$$\text{Cloud factor} = 1 - \frac{K_{in,measured}}{K_{in,potential}} \qquad \text{Eq. 2.2}$$

The last part of the cloud factor Equation 2.2 is calculated from the solar radiation at the top of the atmosphere. This is given by the equation for potential incoming shortwave radiation ($K_{in,\ potential}$) (Moene & van Dam, 2013) (Equation 2.3),

$$K_{in,potential} = \overline{I_0} \left(\frac{\overline{d_{sun}}}{d_{sun}} \right)^2 \cos(\theta_Z) \qquad \text{Eq. 2.3}$$

where I_0 is the solar constant that equals 1365 W/m^2 (flux density of solar radiation at the mean distance from Sun to Earth), d_{sun} (with line over) is the mean distance between the Sun and the Earth over a year, d_{sun} is the actual distance from the Sun to the Earth depending on the date, Θ_Z is the solar zenith angle at the time of measurement (the angle between the solar irradiation and the normal to the Earth's surface depending on the location, date and time). The zenith angle was calculated from solar elevation angle (angle between solar radiation and horizontal) from the sampling scheme that is a complementary angle of the solar zenith angle.

From the Equation 2.3, the ratio can be calculated by Equation 2.4,

$$\left(\frac{\overline{d_{sun}}}{d_{sun}} \right)^2 \qquad \text{Eq. 2.4}$$

can be calculated by Equation 2.5,

$$1 + 0.033\ \cos\left[2\pi * \frac{n_{day}}{365}\right] \qquad \text{Eq. 2.5}$$

where n_{day} is the day of the year, starting from January the first.

The solar radiation at the ground is partly determined by the factors from the top of the atmosphere through the atmosphere down to the ground. Most of the variations in the solar radiation at the ground are due to clouds. Other components in the atmosphere are the content of water vapor that leads to variation in absorption in the atmosphere, and aerosols that can reflect, absorb and scatter radiation. In addition to diurnally variations, the variation in solar radiation can have latitudinal and seasonal variation depending on the location on the

Earth (Moene & van Dam, 2013). Therefore, the zenith angle is an important part of the cloud factor calculation.

Statistical analysis

The influence of the environmental variables influencing the surface albedo was analyzed with a generalized linear mixed model (GLMM) using the glmer function in the R package lme4 (Bates et al., 2015). Measurements on the surfaces were paired and repeated for the same surface. To account for this pseudoreplication, ID (of the surface) was nested in Date (of measurements) as a random variable.

All environmental factors were included in the model. However, to avoid collinearity, only the cloud factor was used to predict the influence of clouds. The Pearson correlation test was used to look for collinearity among variables. This was revealed for cloud cover and cloud factor as they both are ways of measuring the influence of clouds on the surface albedo.

To assess under-dispersion, the R package Dharma (Hartig, 2019) was used to run a dispersion test, as is reported in the appendix (Table A3). A binomial distribution was first considered; however, it did not account for the under-dispersion. A quasibinomial distribution in a generalized linear model (GLM) was then tested, as it did account for the under-dispersion by adding one extra parameter in the distribution. The quasibinomial distribution is a less good way to account for little variance in the data. In addition, a GLM does not account for the pseudoreplication. Another solution was to use beta regression and adding a random component.

Lastly, to account for under-dispersion in the data, a Gamma distribution was used in a GLMM, with log specification (family 0 "Gamma" (link="log")) to run the model. The zenith angle was scaled to be on a proportional scale as the surface albedo and cloud factor. All seven species where included in the model, as well as the four aspect categories.

The mod.sel function in the R package MuMIn was used to find the most suited explanatory variables to best predict the surface albedo (Barton, 2019). All possible combinations of the explanatory variables where explored and where ranked according to the Akaike information criterion controlling for small sample sizes (AICc). The retaining models was ranked and one model with delta AICc < 2 was the supported model (lowest AICs) as the top model that was equally supported by the data (Burnham and Anderson, 2004). Then a 95 % confidence interval (CI) was calculated for the prediction variables. Only predictor variables with 95 % CI spanning zero were considered uninformative (Arnold, 2010). Figures were plotted by using the R package ggplot2 (Wickham, 2016). All data analysis was performed using R version 3.6.0 (R Core Team, 2019).

3. Results

3.1 Difference in surface albedo between species

The surface albedo measurements show that all the surfaces were absorbing more shortwave radiation than they reflected (Figure 1). The mean surface albedo values differed in the reflection between species when all environmental variables were included. All measurements of the surface albedos were influenced by different cloud covers and changing zenith angle at noon. In addition, the two light-colored species *C. stellaris* and *F. nivalis* had the highest surface albedos. They were the only species where albedo was measured with north- and south-facing aspects. For the darker surfaces of *E. nigrum* covers and *C. islandica*, the surface albedo, but also sample size were lower (Figure 1; Table 1).

The amount of reflection of solar radiation decreased respectively from *C. stellaris* (0.36 ± 0.02), *F. nivalis* (0.34 ± 0.02), 25 % *E. nigrum* cover (0.29 ± 0.02), 50 % *E. nigrum* cover (0.23 ± 0.01), 75 % *E. nigrum* cover (0.18 ± 0.02), to 100% *E. nigrum* cover (0.15 ± 0.01) and *C. islandica* (0.15 ± 0.01) (Figure 1; Figure A1; Table 2).

C. stellaris achieved the highest mean (0.36 ± 0.02, range: 0.31 – 0.39) surface albedo, compared to *F. nivalis* (0.34 ± 0.02, range: 0.29 – 0.38). Both species had similar range in surface albedo values. The *C. stellaris* also had the highest individual surface albedo of 0.39. For *F. nivalis* the highest individual surface albedo was 0.38 (Table 2).

The *E. nigrum* surfaces had decreasing albedo with increasing cover of *E. nigrum*, with highest albedos for zero *E. nigrum* cover, and lowest for total coverage. For 25 % cover of *E. nigrum* the mean surface albedo was 0.29 (± 0.02, range: 0.27 – 0.31), and this was similar to the lowest measured surface albedo values for *F. nivalis.* When *E. nigrum* was covering half of the surface, the mean albedo further decreased to 0.23 (± 0.01, range: 0.21 – 0.25). This was lower than any surface albedo measurements with 25 % *E. nigrum* cover. The 75 % *E. nigrum* cover had a mean surface albedo of 0.18 (± 0.02, range: 0.15 – 0.20). The total coverage of *E. nigrum* had a mean surface albedo of 0.15 (± 0.01, range: 0.14 – 0.17), and values were overlapping with the surface albedo measurements for 75 % *E. nigrum* cover (Figure 1; Table 2).

C. islandica is a darker lichen species than *C. stellaris* and *F. nivalis* and it had the lowest individual surface albedo measurement of all the surfaces. The *C. islandica* had a mean surface albedo of 0.15 (± 0.01, range: 0.13 – 0.17) and had similar mean and range as total coverage of *E. nigrum* (Table 2; Figure 1; Figure A1).

The GLMM shows that *F. nivalis* had a slightly lower surface albedo compared to *C. stellaris*. For the other species with increasing darkness in the surface, the surface albedo decreased as expected (Table A3).

3.2 Zenith angle

Only the surface albedo measurements done at noon had a decreasing zenith angle (Figure A5). All the other aspect categories were measured with a constant zenith angle.

The mean surface albedo for *C. stellaris* were 0.34 (± 0.01*)* and for *F. nivalis* it was 0.33 (±0.01) at noon. For both species, these albedos are lower than for the overall mean surface albedo values, and all aspects except north-facing slopes (Table 2).

The GLMM showed that the zenith angle had a small influence on the surface albedo on noon measurements when all species were included (Table A3). This relationship can be seen for *F. nivalis* and *C. stellaris* (Figure 2). *C. stellaris* and all the other darker surfaces had a smaller sample size, which could have resulted in a less accurate influence of zenith angle on the surface albedo. However, the effect of zenith angle on *C. stellaris* measurements showed that the surface albedo was increasing with increasing zenith angle, even with the lower sample size (Figure 2).

The effect of the zenith angle could have been influenced by other environmental factors. The surface albedo measurements of all species measured with increasing zenith angle and horizontal surface at noon, also had changing cloud cover included in the GLMM (Table A3; Figure A3). Cloudiness can lower the influence zenith angle have on the surface albedo and might have influenced the surface albedo measurements at noon. However, there was still an effect of zenith angle (Table A3).

3.3 Aspect

The GLMM showed that aspect influenced the surface albedo when all species were included (Table A3; Figure 3). The influence of aspect categories with constant zenith angle was higher than for a horizontal surface at noon. However, the north- and south-facing slopes did not have a significant effect on the surface albedo (Table A3).

C. stellaris and *F. nivalis* with constant zenith angle had the highest surface albedos at horizontal surfaces in the morning and afternoon, and the lowest surface albedo at north-facing slopes (Table 2). For both the light-colored species, the horizontal surface at noon and north-facing surface were similar in terms of having the lowest mean surface albedo values at these aspects. South-facing surface had similar surface albedo measurements as horizontal surfaces in the morning and afternoon (Table 2; Figure 3).

C. stellaris and *F. nivalis* had the lowest mean surface albedos at noon and north-facing slope, with respectively 0.34 for noon and 0.34 north-facing for *C. stellaris*, and 0.32 for noon and 0.33 north-facing for *F. nivalis* (Table 2). The north-facing slope measurements had the lowest variation in surface albedo measurements for *F. nivalis*. The highest surface albedo measurements were at horizontal surface in morning and afternoon, and south-facing surface for both light colored species. *C. stellaris* measured a mean 0.36 at horizontal surface at morning and afternoon, and 0.37 at south-facing slope (Table 2). *F. nivalis* measured 0.35 at horizontal morning and afternoon and 0.36 at south-facing slope the albedo (Table 2).

3.4 Cloud factor

The GLMM showed that cloud factor influenced the surface albedo (Table A3; Figure 4 – 5). This effect was higher than for the other environmental factors (Table A3). All surface albedo measurements were influenced by changing cloud cover, which can impact the influence the other environmental factors have on the surface albedo. However, most measurements were done at lower cloud factor values and were therefore clustered to the left in Figure 4. The lower sampling of higher cloud factor values also reflected this. Despite this, high surface albedos where observed with high cloud factor values.

Variation in the cloud factor values was higher than variation in the surface albedo measurements for all species (Table 2–3; Figure A4). The low variation in the surface albedo could therefore result in under-dispersion.

For *C. stellaris* and *F. nivalis* the surface albedo decreased with increasing cloud factor (Figure 5). For *C. stellaris* the cloud factor ranged from 0.20 to 0.95 (mean ± SD = 0.36 ± 0.18) (Table 3). For *F. nivalis* the cloud factor ranged from 0.16 to 0.94 (mean ± SD = 0.36 ± 0.17), and also had a larger sample size than for *C. stellaris* (Table 3). *F. nivalis* had more measurements done later in the study period, when more clouds were present. Therefore, the cloud factor was slightly lower for *F. nivalis* than for *C. stellaris*.

C. stellaris had the lowest cloud factor value of 0.20 with surface albedo of 0.37 at south-facing surface, and cloud cover of 3 (Table 2–3). The highest cloud factor value was 0.95, with surface albedo of 0.33 at horizontal surface with constant zenith angle, and cloud cover of 3. *F. nivalis* had the lowest cloud factor value of 0.16, had surface albedo of 0.32 at horizontal surface at noon, and cloud cover of 3 (Table 2–3). The highest cloud factor value was 0.94, with surface albedo of 0.31 at horizontal surface with constant zenith angle, and cloud cover of 3 (Table 2–3).

The surface albedo did not differ much with the changing cloud factor for the darker species. The darker species had a smaller sample size (6 – 12 measurements; Table 1) and did not cover the scale of cloud factor as the light-colored lichen species. The different surfaces had a different range in the cloud factor (Table 3). Since the sample size was low, these few samples could have influential values and therefore not show influence of clouds on the surface albedo as for the light-colored species.

The highest cloud factor values were also represented with the two highest cloud cover categories (Figure A3). The surface albedo can be high despite being high cloud cover observations and high cloud factor values (Figure 4; Figure A3).

Even though cloud factor and cloud cover observations were correlated, they did not fully match the same pattern for influence of clouds on the surface albedo (Figure 4; Figure A3). For instance, low cloud factor and high surface albedo had observations of high cloud cover. Thus, the cloud factor and cloud cover did not correspond, and cloud factor represent another range than cloud cover observations. This showed that cloud factor represented another range than cloud cover observations.

3.5 Cloud cover

The surface albedo decreased with increasing cloud cover (Table A2; Figure 6). Despite this, the cloud cover showed high surface albedo even though cloud cover was observed within the group 2 and 3 (Figure A3). The reflection of solar radiation differed with and without the presence of clouds.

The different cloud cover categories from zero to eight were best represented in *C. stellaris* and *F. nivalis* due to their larger sample size. However, most of the measurements for *C. stellaris* and *F. nivalis* had observations of zero or low cloud cover, and some categories were represented with few cloud cover observations. The other groups had smaller sample sizes, and all the cloud cover categories were not represented in *C. islandica* and all the *E. nigrum* covers (Table A1; Figure A2).

C. stellaris and *F. nivalis* had most measurements done at zero cloud cover, with 51 and 55 observations respectively (Table A2). For cloud factor this was also the trend, where most of the measurements were done under low cloud factor and was clustered to the left (Figure 4).

C. stellaris had higher surface albedo in all the cloud cover categories compared to *F. nivalis*. Both species showed decreasing surface albedo with increasing cloud cover (Table A2). When cloud cover was merged into three groups, the albedo decreased with increasing cloud cover. This was for measurements done with and without constant zenith angle.

For both light-colored species with zero cloud cover, the albedo was higher at horizontal surface in morning and afternoon with constant zenith angle (Table A2). The albedo decreased with increasing cloud cover for both species with and without constant zenith angle. With constant zenith angle, the values were based on a smaller sample size.

The clouds' influence on the highest and lowest surface albedos can be seen in the *C. stellaris*. The species had the lowest albedos of 0.31 and was measured at north-facing surface with cloud cover of 2, and cloud factor of 0.45 (Table 2; Figure 4; Figure A3). The highest albedo value of 0.39 was measured at horizontal surface with constant zenith angle with cloud cover of 1, and cloud factor of 0.31 (Table 2; Figure 4; Figure A3).

For *F. nivalis* the lowest albedo value of 0.29 were measured at horizontal surface at noon, with cloud cover of 2 and cloud factor of 0.45. The highest albedo value was 0.38 for the same species measured at horizontal surface with constant zenith angle and cloud cover of 1, and cloud factor of 0.24 (Table 2; Figure A3).

4. Discussion

The results showed that the two lightest surfaces, *C. stellaris* and *F. nivalis*, reflected more solar radiation than the other surfaces. With increasing cover of *E. nigrum* the surface albedo decreased. The dark lichen *C. islandica* had similar reflection of solar radiation as the total coverage of *E. nigrum*. The surface albedo was also influenced by environmental factors. During the study period the zenith angle, aspect and cloud cover were affecting the reflection of solar radiation. Amongst these factors, clouds had the most influence on the surface albedo. However, the zenith angle and aspect were also explaining the variation in the surface albedo.

4.1 Difference in the surface albedo between species

In this study, all the surface albedo measurements showed that the surfaces absorbed more solar radiation than they reflected. However, the proportion of reflected radiation differed between the surfaces. This difference between lichens and shrubs has also been found by Peltoniemi et al. (2010). The study showed a surface albedo of 0.31 for light-colored lichens compared to 0.20 for lingonberries (*V. vitis-idaea*). Even higher surface albedos for the light-colored lichens have been found by Heim and Lundholm (2013) with mean albedo of 0.33 for *Cladonia* spp. Both these studies show lower values than revealed by the experiment on *C. stellaris* reported in this thesis, and might be due to the presence of *Cladonia rangiferina* used in the other studies with its natural grey color.

The influence of light-colored lichens on the surface albedo has also been the focus for field studies on arctic vegetation. A study by Petzold and Rencz (1975) showed that high coverage of *C. stellaris* gave albedos of 0.20 in heath tundra, 0.22 in shrub heath and 0.26 in coniferous forest. In comparison, other types of vegetation where this lichen was not present, such as meadow vegetation, had surface albedos ranging from 0.16 to 0.18. In the same study, increasing colonization and cover of *C. stellaris* after forest fire led to an increase in the surface albedo. The same has also been revealed in another study by Kershaw (1978) where the highest albedo was for the late colonization of *C. stellaris,* 80 years after fire. These studies show the effect *Cladonia* spp. have in increasing the surface albedo for different vegetation types. The same was also found in this thesis in the experiment with changing the coverage of *E. nigrum* and *C. stellaris*, where decreasing proportion of the light-colored lichen decreased the surface albedo.

The surface albedo of a vegetation type is dependent on the growth forms. Measurements of the surface albedo on vegetation types can be lower than for target species and individual leaves because of the mixture of growth forms (Oke, 1987; Peltoniemi et al., 2010). For instance, vegetation types containing light-colored lichens can have higher surface albedo than vegetation with shrubs and trees where the lichen cover is reduced or not existing (i.e. Beringer et al., 2005; Bernier et al., 2011; Cohen et al., 2013; Williamson et al., 2016). Tundra vegetation consisting of *Cladonia* spp. can have higher surface albedo compared to coniferous forest containing the same lichen, with albedos of respectively 0.19 and 0.10 (Beringer et al., 2005). Along this gradient from tundra vegetation to boreal forest, the increase in biomass and canopy complexity showed a decrease in the reflection of solar radiation (Thompson et al., 2004). However, this effect from the vegetation on the surface albedo does not necessarily change proportionally with increasing biomass and shrub abundance. The surface albedo is dependent on the species composition, the canopy density and its architecture (Betts, 2000; Williamson et al., 2016).

The transition from open lichen vegetation to a closed canopy forest can also affect the local climate with changing the albedo of the vegetated surfaces. A reduction in coniferous forest canopy and increase in the cover of *Cladonia* spp. can have a negative effect on the climate by having a cooling effect in the atmosphere, where more solar radiation is reflected (Bernier et al., 2011). An increase in coniferous trees or other plants with dark-colored foliage, together with reduction in light-colored lichens can thus lead to less reflection of the solar radiation. In this experiment, the transition from zero, to total coverage of *E. nigrum,* resulted in a decrease in the surface albedo. The zero cover of *E. nigrum,* or total coverage of the *C. stellaris* surface, produced the highest albedo value of 0.39. In comparison a total coverage of *E. nigrum* showed a surface albedo of 0.14. This represents a reduction in the reflection of more than half the albedo value for a surface with total coverage of *E. nigrum*. Consequently, a transition from a light-colored lichen-dominated surface to shrub vegetation can potentially substantially impact the energy budget with a decreasing reflection of solar radiation.

The dark *C. islandica* had similar reflection of solar radiation as total coverage of *E. nigrum*. This shows that a darker lichen surface can also reduce the proportion of shortwave radiation reflected back to the atmosphere. The surface albedo may change within the same growth form, and not only between growth forms. A shift in the composition of lichen species can therefore have the same effect on albedo as shrubification in lowering the reflection of radiation at the surface. Despite this, differences in lichens are not fully explored here and other studies on surface albedo in alpine and northern areas have also focused on vegetation containing shrubs.

A species-specific knowledge of the surface albedo has been addressed in the study by Peltoniemi et al. (2010). They stress the urge of systematic measurements from specific surfaces, although, they did not mention what lichen species was used in their analysis. The vegetation data was computed from an earlier study on understory vegetation using a field spectrometer, and presumably *C. rangiferina* and *C. stellaris* were the target species for detecting the surface albedo (Peltoniemi et al., 2005).

Many surface albedo studies on vegetation use few vegetation classes for categorizing different vegetation types. When studies use few vegetation classes, this leads to many growth forms being included in each of the vegetation classes. This can be a drawback when studying satellite images and using few vegetation classes which generalize a highly heterogeneous vegetation containing different growth forms and species (Virtanen and Ek, 2014). As a result, it can be difficult to assess the influence on the surface albedo from different lichen species, and species within other growth forms, when they are represented as one group within a vegetation class. The classification can influence the surface albedo values of the different types. For instance, a vegetation class containing one dominant shrub species can make up coverage in other vegetation classes and influence the surface albedo in the other vegetation classes (Loranty et al., 2011). The coverage of the dominant shrub can lead to less difference between the surface albedo for vegetation classes (Loranty et al., 2011). In addition, different vegetation types can have similar surface albedo. This was found by Blok et al. (2011) for a transition from wetland to shrub vegetation where the surface albedo was not changing, when replacing wetland tundra with shrubs.

Studies on satellite images often use *Cladonia* spp. for detecting vegetation change due to their light color (Tømmervik et al., 2003; Theau et al., 2010). However, at the scales used for satellite images, it can be difficult to distinguish between species and vegetation types (Virtanen and Ek, 2014). For instance, *C. stellaris* grows on heaths with other lichen species that also have a light color such as *F. nivalis* and *A. ochroleuca* (Oksanen and Virtanen, 1995; Bidussi et al., 2016). The two light-colored lichens in my study had similar surface albedo and dividing lichens by color can explain the variation in the surface albedo of vegetation. However, it is also important to report the cover of lichen species, as differences in the surface albedo can be due to traits of specific species.

There are also other factors that can influence the surface albedo. External factors, such as vegetation grazing with removal of light-colored lichens can reduce the reflection of solar radiation at the ground. This has been found in Scandinavia where areas with heavy grazing on *Cladonia* spp. have lower surface albedo than areas with higher lichen cover and less grazing (Stoy et al., 2012; Cohen et al., 2013). In contrast, heaths and exposed ridges with light grazing consisting of dwarf shrubs, such as *E. nigrum*, and lichens, such as *F. nivalis*, *C. stellaris* and *C. islandica,* can have lower surface albedo than similar sites with heavy grazing and strong decline in the lichen and shrub coverage (Oksanen and Virtanen, 1995; Beest et al., 2016). This trend is restricted to areas with heavy reduction in lichens. After heavy grazing, lichens cover can have a rapid recovery of 60 % after 7 years (Tømmervik et al., 2012), which is contrary to Kumpula et al. (2000) who found a full recovery of the lichens after 18 years. Recovery can then again lead to new albedo dynamics at the ground.

Another factor that might influence surface albedo measurement is surrounding elements and vegetation. However, in my experiment there was a buffer zone to account for this. In the study by Petzold and Rencz (1975) it was mentioned that dwarf birch (*B. nana*) stands nearby the measurement plots, which potentially could have influenced the measurements. This is the drawback when measuring the surface albedo in the field, with taller vegetation, such as trees and shrubs, being present. Surrounding vegetation can cause shading for the incoming solar radiation depending on the position of the sun that changes diurnally.

The roughness of a surface is another influential factor on surface albedo measurements. Pictures from the surface albedo experiment of Heim and Lundholm (2013) showed uneven surfaces of the *C. stellaris* lichens, and uneven structure could have shaded the surfaces. For more accurate measurements it is important to maintain a heterogeneous horizontal surface, as shading can lower the surface albedo. In my experiment, the lichens were placed as horizontal as possible to prevent shading. For measurements done in the field, it is difficult to measure totally horizontal surfaces due to variations in the landscape shape. However, these disturbances are difficult to avoid, as vegetation can be highly heterogeneous in terms of growth forms and due to the topography.

The ability of lichens to absorb water was not considered in this experiment, even though it might be influencing the surface albedo. They can absorb water and thus increase their biomass. Lichen water content is related to the varying climatic conditions and can dry up completely in sunshine, but the water content can also quickly increase with increasingly humid weather (Matwiejuk, 2000). In addition, lichens can change color when wet, and this might influence the albedo as well (Palmquist and Sundberg, 2000).

4.2 Zenith angle

In my experiment, the surface albedo increased with higher solar zenith angle for *F. nivalis* (Figure A5). The same pattern can be seen for *C. stellaris*; however, it had fewer measurements and could therefore have influenced the prediction of the zenith angle. The increasing zenith angle for horizontal surface at noon (over the measurement period) resulted in increasing surface albedo. This shows that the seasonal variation in the zenith angle is an important factor that can affect the surface albedo. The same pattern has also been found by Peltoniemi et al. (2010) with a weak positive relationship of the surface albedo and zenith angle on *Cladonia* spp. lichens. Also, the surface albedo of white, snow-covered surfaces has the same influence from the zenith angle (Pirazzini, 2004; Sedlar et al., 2011).

For alpine ecosystems in the northern areas, the solar zenith angle changes greatly diurnally and seasonally. With lower zenith angle, the incoming sunlight can penetrate deeper into the structure of a surface and the radiation can be trapped, and at higher zenith angle more of the incident light is reflected from the same surface (Pirazzini, 2004). At an ideal site, the incoming solar radiation is controlled by the azimuth and zenith angle of the sun relative to the horizon, with maximum incoming shortwave radiation at local solar noon (Oke, 1987). Since the zenith angle changes greatly through the day, studies report the time of the day for surface albedo measurements. This makes it easier to assess the influence of the zenith angle in these studies.

The effect from the zenith angle decreases with increasing cloud cover. The shortwave shading effect from clouds increases as the sun rises in the sky, and in months with sunlight the shading effect from clouds is strongest at solar noon (Shupe and Intrieri, 2004). With overcast conditions, the influence from zenith angle on the surface albedo is less since more of the incoming solar radiation is hitting atmospheric components such as clouds (Oke, 1987, Pirazzini, 2004, Shupe and Intrieri, 2004, Bennie et al., 2008). In this study, the surface albedo for *C. stellaris* and *F. nivalis* showed a lower effect from the zenith angle than the influence from the cloud factor. This might be due to the clouds lowering the effect of the zenith angle. The cloud effect can give influential data points for the influence of zenith angle on the surface albedo, and especially for *C. stellaris* that had a lower sample size than *F. nivalis*.

4.3 Aspect

In this study, the surface albedo of *C. stellaris* and *F. nivalis* was influenced by different aspects. As expected, the north-facing slopes showed lower surface albedo than the horizontal and south-facing surface for both species. Under cloudless conditions, in the Northern Hemisphere a north-facing slope receives less radiation than a south-facing slope during midday (Oke, 1987; Bennie et al., 2008). Therefore, the north-facing surfaces in my experiments were influenced by less radiation and more shading than the other aspects due to the orientation of the surfaces. Oliphant et al. (2003) found that one of the most important factors influencing the surface energy is the orientation and the angle of the slope that are controlling the direct incoming shortwave radiation. For horizontal surface in the morning and afternoon, and south-facing surfaces in this study the surface albedo was greater than for the north-facing surface. This has also been found with satellite studies in Norway, where the surface albedo was higher on south-facing slopes than flat terrain and north-facing slopes (Cherubini et al., 2017).

The topographical variations are important for the radiation budget at local levels that additionally can be influenced by other environmental factors such as clouds (Oke, 1987; Bennie et al., 2008). In this study, measurements with different aspects were influenced by changing cloud cover. More clouds lead to less variation in the diurnal pattern in the surface albedo, and the variation between surfaces can therefore be less (Bennie et al., 2008).

The albedos of vegetated surfaces have also been studied with different aspect and vegetation types. Young et al. (1997) studied the surface albedo of different vegetation types and bare ground with different aspects of the surfaces, for south-, north-, east- and west-facing slopes. Cloudy conditions made the variation between sites even less. However, the influence of aspects is difficult to assess as the study by Young et al. (1997) compared different vegetation types with the same aspects. The same was done in a study by Konzelmann et al. (1997) who did not find any difference in surface albedo on north-facing and horizontal surfaces in the Alps between two different vegetation types. Vegetation types can have different surface albedo, and it is therefore important to compare the same type of vegetation with different aspect categories to assess the influence of aspect. In this experiment, measurements were done repeatedly at the same surface for different aspects.

The incoming radiation can also affect the distribution of vegetation in alpine areas. For instance, the Fennoscandian treeline is higher on the south-west facing slopes that receives more solar radiation and are characterized with higher temperatures, than north-west slopes (Odland, 1996). In addition, species richness has been found to increase with increasing temperature in Norway, with highest richness in topographically rough sites, compared to horizontal terrain (Opedal et al., 2015). This influence from the radiation can influence the distribution and composition of lichens, shrubs and trees in alpine areas.

4.4 Cloud factor and cloud cover

The results in this study, the increasing cloud factor reduced the surface albedo. Most of the measurements were done under lower cloud factors and resulted in higher surface albedo values. With increasing cloud factor the amount of direct incoming solar radiation decreases, and therefore the albedo of a surface is reduced (Oke, 1987; Ramanathan et al., 1989). Clouds are considered one of the most important factors that are influencing the amount of solar radiation that reaches the ground (Ramanathan et al., 1989; Sedlar et al., 2011; Moene & Dam, 2013). Stephens et al. (2015) found that the shading effect of clouds in the Northern Hemisphere on brighter snow surfaces can be up to fifty percent.

When a bright surface is replaced by a darker one, less shortwave radiation is being reflected by the surface under clear skies (Shupe and Intrieri, 2004). In the arctic, warming has been detected at the surface due to loss of ice, despite increases in cloud cover and their optical thickness (Miller and Russell, 2002). This shows that changing surfaces are also controlling the surface albedo dynamics despite increased cloudiness. A vegetation change from lichen heaths to shrubs can therefore reduce the reflection during summer, even with increasing cloud cover.

Future cloud cover regimes can potentially influence the surface albedo dynamics and control the incoming shortwave radiation. At higher latitudes the influence on the surface albedo from clouds and the contribution of these new regimes will be characterized by the potential of increased cloud cover (Folland et al., 2009; Chen et al., 2011; Vavrus et al., 2011).

The influence clouds have on the surface albedo is also dependent on the cloud's physical structure, with a combination of the cloud's temperature, height and content of liquid water (Minnett, 1999; Shupe and Intrieri, 2004; Sedlar et al., 2011). Clouds containing liquid have a greater effect on the incoming shortwave radiation, and can have a cooling effect, compared to ice-only clouds that have little shortwave shading effect (Shupe and Intrieri, 2004). The liquid clouds contain many small droplets and have a greater surface area per volume, than ice-only clouds, with higher optical depth and lower transmittance (Shupe and Intrieri, 2004). These differences in the clouds physical building can be difficult to assess by cloud cover observations. Therefore, the calculations from the cloud factor can be a better measure for the influence on the surface albedo.

Some regions can have a reduction in the incoming shortwave radiation even though the cloud cover is not increasing. This is due to more air pollution and biomass burning that reduce the amount of incoming radiation (Li, 1998). This shows the importance of estimating the effect of all components (clouds, dust, other particles) from the top of the atmosphere and down to the surface, as aerosols are also a contributing part to the cloud factor (Equation 2.2). The total effect might not be visible with cloud cover observations.

In my study, the effect of the cloud factor on the surface albedo was higher than the effect of the solar zenith angle. Also, the effect by the zenith angle was lowered when clouds are present (Shupe and Intrieri, 2004). This might imply that clouds, and atmospheric contents, can have a greater effect on the surface albedo than other environmental factors.

Future studies on the albedo of vegetation surfaces should report the cloud cover to assess the influence of environmental factors on the albedo. This is also addressed by Eugster et al. (2000), who point to the need of albedo measurements that differ between clouds and clear sky measurements, as clouds can lower the incoming solar radiation. Other studies also mention this, as clouds are one of many factors that can explain the variation in the surface albedo (i.e. Oliphan et al., 2003; Loranty et al., 2014; Curry et al., 1996).

My cloud cover observations showed that the surface albedo of the two light lichens decreased with increasing cloudiness. However, most of the measurements were done under lower or no cloud cover observations. Also, surface albedo measurements showed that the albedo can be high despite that the cloud cover observations and the cloud factor is high. Even though cloud factor and cloud cover correlate, a low cloud factor value can have a high cloud cover observation. For instance, clouds that were observed might not shade for the incoming radiation. Also, the influence of observed clouds might depend on the thickness of the clouds.

The cloud cover can change rapidly, and the reduction of shortwave radiation reaching the ground can be greatly reduced within short time periods (Oke, 1987). Cloud cover was observed only one time during 30 minutes of surface albedo measurements, rapid fluctuations in the cloud cover were therefore not considered. This is included in the cloud factor where the incoming radiation is part of the individual cloud factor calculations. The variation in the shortwave radiation can also be seen as fluctuations when plotting the surface albedo during one day of measurements (Oke, 1987).

4.5 Future predictions of vegetation change

The species studied in this experiment can potentially be influenced by future climate change. Lichens in alpine areas show a negative effect to climate warming and might be replaced by an increasing cover of vascular plants (Walker et al., 2006; Klanderud, 2008; Dawes et al., 2011; Elmendorf et al., 2012; Fraser et al., 2014). Lichens are thus responding negatively to the recent increase of *E. nigrum* cover in northern Fennoscandia (Wilson and Nilsson, 2009; Vanneste et al., 2017; Vuorinen et al., 2017; Maliniemi et al., 2018). However, *E. nigrum* is also responding negatively to climate change, resulting in a longer growing season with an increase in frost earlier in the season (Wipf et al., 2009). On the other hand, a short-term experiment showed that evergreen shrubs had little response to induced warming and increased growing season length (Livensperger et al., 2016). This implies that responses to climate change in one species can differ, and future vegetation change is depending on the site.

Vegetation can also influence the climate. In my experiment, the change from light-colored lichens to total coverage of *E. nigrum* can more than halve the albedo of a vegetated surface. This can be coupled to the recent increase in shrubs at the expense of light-colored lichens (Fraser et al., 2014). Such a transition can therefore lead to reduced reflection of solar radiation and a positive feedback on the climate. This has also been addressed in observational studies on increased shrub cover in northern parts of Alaska (Sturm et al., 2001; Chapin III et al., 2005; Tape et al., 2006). More absorption of solar radiation is thus transformed into thermal energy that warms the vegetated surface (Oke, 1987).

Increased cover of shrubs and trees are predicted to continue in alpine and northern areas, and this can lead to new surface albedo dynamics (Pearson et al., 2013; de Wit et al., 2014; Mod and Luoto, 2016). Future climate warming in these areas can drive further vegetation changes and lengthening of the growing season (Schwartz et al., 2006; Pearson et al., 2013; Ernakovich et al., 2014). A longer snow-free season can lead to more absorption of solar radiation at the ground due to less snow cover (Chapin III et al., 2005). In addition, the increased cover of shrubs and trees with branches above the snow pack can absorb solar radiation and further speed up the snowmelt (Sturm et al., 2005; Pomeroy et al., 2006; Loranty et al., 2011; Bonfils et al., 2012; Cohen et al., 2013; Loranty et al., 2014; Beest et al.; 2016). This can give an increase the surface albedo earlier in the season during snow melt and lead more ground warming earlier in the spring.

The shrubification can have an indirect insulation and warming effect on the ground by trapping of snow (Sturm et al., 2005; Wookey et al., 2009; Myers-Smith et al., 2011) and this can negatively affect lichens cover as soil warming facilitates further shrubification (Wookey et al., 2009; Myers-Smith et al., 2011). A warmer surface promotes roots to penetrate deeper into the soil and can decrease the cover of lichens and can lead to permafrost thaw (Lawrence & Swenson, 2011; Pearson et al., 2013). The increased warming thus leads to more competition between lichens and vascular plants.

In addition, new precipitation regimes are also predicted (IPCC, 2013). Areas with increased snow fall can negatively affect lichens that are associated to grow at locations with thin or lacking snow cover (Bruun et al., 2006; Löffler, 2007; Odland and Munkejord, 2008; Bidussi et al., 2016). *F. nivalis* is one species that thrives on exposed ridges and can be negatively affected new precipitation regimes (Bidussi et al., 2016). Warmer winters and more rain can increase ground icing events that for example *Cladonia* spp. can be sensitive to (Bjerke, 2011).

Lichens have the ability to affect the climate. By reducing the distribution of lichens, their cooling effect in their environment can be less (Porada et al., 2016). Studies show a different effect of lichens on the ground. Stoy et al. (2012) found higher surface albedo and surface temperature on *Cladonia* spp. than other vegetation. A reduction in lichen cover lowers the surface temperature, due to an increase in ground heating and reduction in latent and sensible heat flux, that decrease the transport of heat from the lichen surface (Stoy et al., 2012). Another study by Kershaw (1978) found cold soil temperature under *C. stellaris* mats that restricted growth of vascular plants. During summer, the reduced soil temperatures under lichens can thus lead to a negative feedback on a local scale (Bernier et al., 2011; Porada et al., 2016).

On the other hand, shrubs can also reduce the soil temperature despite having a lower surface albedo than lichens. Taller shrubs can have a shading effect where less solar radiation penetrates the ground and the understory vegetation (Blok et al., 2010; Bernier et al., 2011). The taller shrubs can thus have a cooling effect on the climate by shading and reduce permafrost thaw (Blok et al., 2011; Lawrence and Swenson; 2011). For instance, Chapin III et al. (2005) studied absorption of solar radiation of forest tundra that had lower surface albedo than other arctic vegetation due to trapping of shortwave radiation. Despite this shading effect, Bonfils et al. (2012) found that a decrease in the surface albedo on northern latitudes with increase in taller shrubs can give warmer soils, increase in destabilization of permafrost and atmospheric heating. The shrubs effect is complex and should be incorporated with the effect from other growth forms to understand the energy budget at the ground.

Future predictions of vegetation change can reduce the distribution of lichens in alpine areas. These changes can therefore lead to new albedo dynamics at the ground, and eventually the Earths radiation budget. Vegetation change has an influence on the energy budget both globally (Duveiller et al., 2018), and regionally (Sturm et al., 2001). The albedo changes due to land use show a negative radiative forcing (i.e. having a cooling effect) with medium level of confidence (IPCC, 2013). At a regional scale, however, the radiative forcing from increased length on the snow free season have contributed to more warming than the atmospheric CO_2 (Chapin III et al., 2005). A longer growing season can give an earlier increase in sensible heating of the atmosphere. This can be amplified by a decrease in lichen cover and an increase in shrubs.

5. Conclusion

In this MSc thesis project, I performed surface albedo measurements on three lichens species and one shrub species. The experiment was run in Bø, South-Eastern Norway, in April to June 2019. In addition, the impact of environmental factors that influence the solar radiation was studied. The conclusion is based on the aims of this experiment:

1) **What is the surface albedo of three lichen species *F. nivalis, C. stellaris*, and *C. islandica*, and the evergreen low growing shrub, *E. nigrum*?** The surface albedo differed between species of different colors, decreasing respectively for *C. stellaris* (0.36), *F. nivalis* (0.34), 25 % *E. nigrum* (0.29), 50 % *E. nigrum* (0.23), 75 % *E. nigrum* (0.18), 100 % *E. nigrum* (0.15) and *C. islandica* (0.15). Lichen species with the same color had similar surface albedo. Also, different growth forms can have similar surface albedo such as *C. islandica* and total coverage of *E. nigrum*.
2) **What is the impact of the solar zenith angle, aspect and cloud cover on the surface albedo?** The surface albedo decreased with decreasing zenith angle. For the north-facing slope the surface albedo was lower, compared to the other aspects. With increasing cloudiness, the surface albedo also decreased, and the effect was highest for this factor than for the others environmental factors. For both the zenith angle and aspect the influence on the surface albedo decrease with increasing cloudiness.

Vegetation in alpine areas is changing. A small change in the surface albedo can influence the energy budget at the ground. Therefore, the influence of species surface albedo is important to understand. Environmental factors that influence the variation in the albedo of a vegetated surface should be included in future studies. This information can give more accurate predictions of the surface albedo of vegetation for future projections of climate change.

Future studies on surface albedo of vegetation should report cloudiness and time of the day. In addition, for assessing the influence of aspect on the surface albedo it is important to compare the same type of vegetation for different aspects. Also, the coverage of different species should be reported to understand species contribution in affecting the surface albedo.

6. References

Ahti, T., and J. Oksanen. 1990. Epigeic lichen communities of taiga and tundra regions. Vegetatio **86**:39-70.

Arnold, T. W. 2010. Uninformative Parameters and Model Selection Using Akaike's Information Criterion. The Journal of Wildlife Management **74**:1175-1178.

Barton, K. (2019). MuMIn: Multi-Model Inference. R package version 1.43.15. Retrieved from https://CRAN.R-project.org/package=MuMIn

Bates, D., Maechler, M., Bolker, B., Walker, S. (2015). Fitting Linear Mixed-Effects Models Using lme4. Journal of Statistical Software, **67**(1), 1-48. doi:10.18637/jss.v067.i01.

Beest, M. t., J. Sitters, C. Ménard, B. , and J. Olofsson. 2016. Reindeer grazing increases summer albedo by reducing shrub abundance in Arctic tundra. Environmental Research Letters **11**:125013.

Bennie, J., B. Huntley, A. Wiltshire, M. O. Hill, and R. Baxter. 2008. Slope, aspect and climate: Spatially explicit and implicit models of topographic microclimate in chalk grassland. Ecological Modelling **216**:47-59.

Beringer, J., F. S. Chapin, C. C. Thompson, and A. D. McGuire. 2005. Surface energy exchanges along a tundra-forest transition and feedbacks to climate. Agricultural and Forest Meteorology **131**:143-161.

Bernier, P. Y., R. L. Desjardins, Y. Karimi-Zindashty, D. Worth, A. Beaudoin, Y. Luo, and S. Wang. 2011. Boreal lichen woodlands: A possible negative feedback to climate change in eastern North America. Agricultural and Forest Meteorology **151**:521-528.

Betts, R. A. 2000. Offset of the potential carbon sink from boreal forestation by decreases in surface albedo. Nature **408**:187-190.

Bidussi, M., K. A. Solhaug, and Y. Gauslaa. 2016. Increased snow accumulation reduces survival and growth in dominant mat-forming arctic-alpine lichens. The Lichenologist **48**:237-247.

Bienau, M. J., Kröncke, M., Eiserhardt, W. L., Otte, A., Graae, B. J., Hagen, D., ... & Eckstein, R. L. (2015). Synchronous flowering despite differences in snowmelt timing among habitats of Empetrum hermaphroditum. Acta Oecologica, 69, 129-136.

Bjerke, J. W., & Elvebakk, A. (2004). Distribution of the lichen genus Flavocetraria (Parmeliaceae, Ascomycota) in the Southern Hemisphere. New Zealand Journal of Botany, 42(4), 647-656.

Bjerke, J. W. 2011. Winter climate change: Ice encapsulation at mild subfreezing temperatures kills freeze-tolerant lichens. Environmental and Experimental Botany **72**:404-408.

Blok, D., Heijmans, M. M., SCHAEPMAN-STRUB, G., Kononov, A. V., Maximov, T. C., & Berendse, F. (2010). Shrub expansion may reduce summer permafrost thaw in Siberian tundra. *Global Change Biology*, *16*(4), 1296-1305.

Blok, D., G. Schaepman-Strub, H. Bartholomeus, M. M. P. D. Heijmans, T. C. Maximov, and F. Berendse. 2011. The response of Arctic vegetation to the summer climate: relation between shrub cover, NDVI, surface albedo and temperature. Environmental Research Letters **6**:035502.

Bonfils, C. J. W., T. J. Phillips, D. M. Lawrence, P. Cameron-Smith, W. J. Riley, and Z. M. Subin. 2012. On the influence of shrub height and expansion on northern high latitude climate. Environmental Research Letters **7**:015503.

Bruun, H. H., J. Moen, R. Virtanen, J. A. Grytnes, L. Oksanen, and A. Angerbjorn. 2006. Effects of altitude and topography on species richness of vascular plants, bryophytes and lichens in alpine communities. Journal of Vegetation Science **17**:37-46.

Bryn, A., G.-H. Strand, M. Angeloff, and Y. Rekdal. 2018. Land cover in Norway based on an area frame survey of vegetation types. Norsk Geografisk Tidsskrift - Norwegian Journal of Geography **72**:131-145.

Burnham, K. P., and D. R. Anderson. 2004. Multimodel Inference: Understanding AIC and BIC in Model Selection. Sociological Methods & Research **33**:261-304.

Cannone, N., S. Sgorbati, and M. Guglielmin. 2007. Unexpected impacts of climate change on alpine vegetation. Frontiers in Ecology and the Environment **5**:360-364.

Carlson, B. Z., M. C. Corona, C. Dentant, R. Bonet, W. Thuiller, and P. Choler. 2017. Observed long-term greening of alpine vegetation—a case study in the French Alps. Environmental Research Letters **12**:114006.

Chapin III, F. S., J. T. Randerson, A. D. McGuire, J. A. Foley, and C. B. Field. 2008. Changing feedbacks in the climate–biosphere system. Frontiers in Ecology and the Environment **6**:313-320.

Chapin III, F. S., M. Sturm, M. C. Serreze, J. P. McFadden, J. R. Key, A. H. Lloyd, A. D. McGuire, T. S. Rupp, A. H. Lynch, J. P. Schimel, J. Beringer, W. L. Chapman, H. E. Epstein, E. S. Euskirchen, L. D. Hinzman, G. Jia, C. L. Ping, K. D. Tape, C. D. Thompson, D. A. Walker, and J. M. Welker. 2005. Role of land-surface changes in arctic summer warming. Science **310**:657-660.

Chen, Y., J. R. Miller, J. A. Francis, and G. L. Russell. 2011. Projected regime shift in Arctic cloud and water vapor feedbacks. Environmental Research Letters **6**:044007.

Cherubini, F., S. Vezhapparambu, W. Bogren, R. Astrup, and A. H. Strømman. 2017. Spatial, seasonal, and topographical patterns of surface albedo in Norwegian forests and cropland. International Journal of Remote Sensing **38**:4565-4586.

Cohen, J., J. Pulliainen, C. B. Menard, B. Johansen, L. Oksanen, K. Luojus, and J. Ikonen. 2013. Effect of reindeer grazing on snowmelt, albedo and energy balance based on satellite data analyses. Remote Sensing of Environment **135**:107-117.

Cornelissen, J. H., S. I. Lang, N. A. Soudzilovskaia, and H. J. During. 2007. Comparative cryptogam ecology: a review of bryophyte and lichen traits that drive biogeochemistry. Ann Bot **99**:987-1001.

Cornelissen, J. H. C., T. V. Callaghan, J. M. Alatalo, A. Michelsen, E. Graglia, A. E. Hartley, D. S. Hik, S. E. Hobbie, M. C. Press, C. H. Robinson, G. H. R. Henry, G. R. Shaver, G. K. Phoenix, D. Gwynn Jones, S. Jonasson, F. S. Chapin, U. Molau, C. Neill, J. A. Lee, J. M. Melillo, B. Sveinbjörnsson, and R. Aerts. 2001. Global change and arctic ecosystems: is lichen decline a function of increases in vascular plant biomass? Journal of Ecology **89**:984-994.

Curry, J. A., Schramm, J. L., Rossow, W. B., & Randall, D. (1996). Overview of Arctic cloud and radiation characteristics. *Journal of Climate*, *9*(8), 1731-1764.

Dawes, M. A., F. Hagedorn, T. Zumbrunn, I. T. Handa, S. Hattenschwiler, S. Wipf, and C. Rixen. 2011. Growth and community responses of alpine dwarf shrubs to in situ CO(2) enrichment and soil warming. New Phytol **191**:806-818.

de Wit, H. A., A. Bryn, A. Hofgaard, J. Karstensen, M. M. Kvalevag, and G. P. Peters. 2014. Climate warming feedback from mountain birch forest expansion: reduced albedo dominates carbon uptake. Glob Chang Biol **20**:2344-2355.

Den Herder, M., M.-M. Kytöviita, and P. Niemelä. 2003. Growth of reindeer lichens and effects of reindeer grazing on ground cover vegetation in a Scots pine forest and a subarctic heathland in Finnish Lapland. Ecography **26**:3-12.

Duveiller, G., J. Hooker, and A. Cescatti. 2018. The mark of vegetation change on Earth's surface energy balance. Nature Communications **9**:679.

Elmendorf, S. C., G. H. R. Henry, R. D. Hollister, R. G. Bjork, N. Boulanger-Lapointe, E. J. Cooper, J. H. C. Cornelissen, T. A. Day, E. Dorrepaal, T. G. Elumeeva, M. Gill, W. A. Gould, J. Harte, D. S. Hik, A. Hofgaard, D. R. Johnson, J. F. Johnstone, I. S. Jonsdottir, J. C. Jorgenson, K. Klanderud, J. A. Klein, S. Koh, G. Kudo, M. Lara, E. Levesque, B. Magnusson, J. L. May, J. A. Mercado-Diaz, A. Michelsen, U. Molau, I. H. Myers-Smith, S. F. Oberbauer, V. G. Onipchenko, C. Rixen, N. M. Schmidt, G. R. Shaver, M. J. Spasojevic, P. E. Porhallsdottir, A. Tolvanen, T. Troxler, C. E. Tweedie, S. Villareal, C. H. Wahren, X. Walker, P. J. Webber, J. M. Welker, and S. Wipf. 2012a. Plot-scale evidence of tundra vegetation change and links to recent summer warming. Nature Climate Change **2**:453-457.

Ernakovich, J. G., K. A. Hopping, A. B. Berdanier, R. T. Simpson, E. J. Kachergis, H. Steltzer, and M. D. Wallenstein. 2014. Predicted responses of arctic and alpine ecosystems to altered seasonality under climate change. Global change biology **20**:3256-3269.

Eugster, W., W. R. Rouse, R. A. Pielke Sr, J. P. McFadden, D. D. Baldocchi, T. G. F. Kittel, F. S. Chapin, G. E. Liston, P. L. Vidale, E. Vaganov, and S. Chambers. 2000. Land-atmosphere energy exchange in Arctic tundra and boreal forest: available data and feedbacks to climate. Global change biology **6**:84-115.

Felde, V. A., J. Kapfer, and J. A. Grytnes. 2012. Upward shift in elevational plant species ranges in Sikkilsdalen, central Norway. Ecography **35**:922-932.

Folland, C. K., J. Knight, H. W. Linderholm, D. Fereday, S. Ineson, and J. W. Hurrell. 2009. The Summer North Atlantic Oscillation: Past, Present, and Future. Journal of Climate **22**:1082-1103.

Fraser, R. H., T. C. Lantz, I. Olthof, S. V. Kokelj, and R. A. Sims. 2014. Warming-Induced Shrub Expansion and Lichen Decline in the Western Canadian Arctic. Ecosystems **17**:1151-1168.

Gaare, E., H. Tømmervik, and S. A. Hoem. 2005. Reinens beiter på Hardangervidda. Utviklingen fra 1988 til 2004. NINA Rapport **53**:20.

Graglia, E., S. Jonasson, A. Michelsen, I. K. Schmidt, M. Havstrom, and L. Gustavsson. 2001. Effects of environmental perturbations on abundance of subarctic plants after three, seven and ten years of treatments. Ecography **24**:5-12.

Hanssen-Bauer I. , F. E. J., Haddeland I. , Hisdal H. , Mayer S. , Nesje A. , Nilsen J. E. Ø. , Sandven S. , Sandø A. B. , Sorteberg A. og Ådlandsvik B. 2015. Kunnskapsgrunnlag for klimatilpasning oppdatert i 2015.*in* Miljødirektoratet, editor.

Hartig, F. (2019). DHARMa: Residual Diagnostics for Hierarchical (Multi-Level / Mixed) Regression Models. R package version 0.2.6. Retrieved from https://CRAN.R-project.org/package=DHARMa

Hauck, M. (2009). Global warming and alternative causes of decline in arctic-alpine and boreal-montane lichens in North-Western Central Europe. *Global Change Biology*, *15*(11), 2653-2661.

Heim, A., and J. Lundholm. 2013. *C. stellaris* lichens on extensive green roofs: evapotranspiration, substrate temperature, and albedo. F1000Res **2**:274.

Ims Vistnes, I., and C. Nellemann. 2008. Reindeer Winter Grazing in Alpine Tundra: Impacts on Ridge Community Composition in Norway. Arctic, Antarctic, and Alpine Research **40**:215-224.

IPCC. 2013. Summary for Policymakers.*in* T. F. Stocker, D. Qin, G.-K. Plattner, M. Tignor, S.K. Allen, J. Boschung, A. Nauels, Y. Xia, V. Bex and P.M. Midgley (eds.), editor. Climate Change 2013: The Physical Science Basis. Contribution of Working Group I to the Fifth Assessment Report of the Intergovernmental Panel on Climate Change, Cambridge University Press, Cambridge, United Kingdom and New York, NY, USA.

Jagerbrand, A. K., K. E. M. Lindblad, R. G. Bjork, J. M. Alatalo, and U. Molau. 2006. Bryophyte and lichen diversity under simulated environmental change compared with observed variation in unmanipulated alpine tundra. Biodiversity and Conservation **15**:4453-4475.

Jonasson, S. 1992. Plant-Responses to Fertilization and Species Removal in Tundra Related to Community Structure and Clonality. Oikos **63**:420-429.

Juszak, I., A. M. Erb, T. C. Maximov, and G. Schaepman-Strub. 2014. Arctic shrub effects on NDVI, summer albedo and soil shading. Remote Sensing of Environment **153**:79-89.

Kershaw, K. A. 1978. The Role of Lichens in Boreal Tundra Transition Areas. The Bryologist **81**:294-306.

Kim, D., and V. Ramanathan. 2008. Solar radiation budget and radiative forcing due to aerosols and clouds. Journal of Geophysical Research: Atmospheres **113**.

Kipp & Zonen B.V. (2014). CNR 4 net Radiometer. Instruction Manual. Manual version: 1409. Retrieved from https://www.kippzonen.com/Product/85/CNR4-Net-Radiometer#.XkEohmhKg2w

Klanderud, K. 2008. Species-specific responses of an alpine plant community under simulated environmental change. Journal of Vegetation Science **19**:363-372.

Klanderud, K., and H. J. B. Birks. 2003. Recent increases in species richness and shifts in altitudinal distributions of Norwegian mountain plants. Holocene **13**:1-6.

Konzelmann, T., P. Calanca, G. Müller, L. Menzel, and H. Lang. 1997. Energy Balance and Evapotranspiration in a High Mountain Area during Summer. Journal of Applied Meteorology **36**:966-973.

Kullman, L. 2002. Rapid recent range-margin rise of tree and shrub species in the Swedish Scandes. Journal of Ecology **90**:68-77.

Kumpula, J., A. Colpaert, and M. Nieminen. 2000. Condition, potential recovery rate, and productivity of lichen (*C. stellaris* spp.) ranges in the Finnish reindeer management area. Arctic **53**:152-160.

Lang, S. I., J. H. C. Cornelissen, G. R. Shaver, M. Ahrens, T. V. Callaghan, U. Molau, C. J. F. Ter Braak, A. Holzer, and R. Aerts. 2012. Arctic warming on two continents has consistent negative effects on lichen diversity and mixed effects on bryophyte diversity. Global change biology **18**:1096-1107.

Lawrence, D. M., and S. C. Swenson. 2011. Permafrost response to increasing Arctic shrub abundance depends on the relative influence of shrubs on local soil cooling versus large-scale climate warming. Environmental Research Letters **6**:045504.

Li, Z. 1998. Influence of Absorbing Aerosols on the Inference of Solar Surface Radiation Budget and Cloud Absorption. Journal of Climate **11**:5-17.

Livensperger, C., Steltzer, H., Darrouzet-Nardi, A., Sullivan, P. F., Wallenstein, M., & Weintraub, M. N. (2016). Earlier snowmelt and warming lead to earlier but not necessarily more plant growth. *AoB Plants*, *8*.

Loranty, M. M., L. T. Berner, S. J. Goetz, Y. Jin, and J. T. Randerson. 2014. Vegetation controls on northern high latitude snow-albedo feedback: observations and CMIP5 model simulations. Glob Chang Biol **20**:594-606.

Loranty, M. M., S. J. Goetz, and P. S. A. Beck. 2011. Tundra vegetation effects on pan-Arctic albedo. Environmental Research Letters **6**:024014.

Löffler, J. 2007. The influence of micro-climate, snow cover, and soil moisture on ecosystem functioning in high mountains. Journal of Geographical Sciences **17**:3-19.

Maliniemi, T., J. Kapfer, P. Saccone, A. Skog, and R. Virtanen. 2018. Long-term vegetation changes of treeless heath communities in northern Fennoscandia: Links to climate change trends and reindeer grazing. Journal of Vegetation Science **29**:469-479.

Marmor, L., T. Torra, L. Saag, and T. Randlane. 2012. Species richness of epiphytic lichens in coniferous forests: the effect of canopy openness. Annales Botanici Fennici **49**:352-358.

Matwiejuk, A. 2000. Water content in terricolous lichens. Acta Societatis Botanicorum Poloniae **69**:55-63.

Michelsen, O., A. O. Syverhuset, B. Pedersen, and J. I. Holten. 2011. The impact of climate change on recent vegetation changes on Dovrefjell, Norway. Diversity **3**:91-111.

Miller, J. R., and G. L. Russell. 2002. Projected Impact of Climate Change on the Energy Budget of the Arctic Ocean by a Global Climate Model. Journal of Climate **15**:3028-3042.

Minnett, P. J. 1999. The Influence of Solar Zenith Angle and Cloud Type on Cloud Radiative Forcing at the Surface in the Arctic. Journal of Climate **12**:147-158.

Mod, H. K., and M. Luoto. 2016. Arctic shrubification mediates the impacts of warming climate on changes to tundra vegetation. Environmental Research Letters.

Moene, F., van Dam, J., C. (2013). Atmosphere – Vegetation – Soil Interactions (p. 16-18). MAQ-22806. Wageningen.

Myers-Smith, I. H., B. C. Forbes, M. Wilmking, M. Hallinger, T. Lantz, D. Blok, K. D. Tape, M. Macias-Fauria, U. Sass-Klaassen, E. Lévesque, S. Boudreau, P. Ropars, L. Hermanutz, A. Trant, L. S. Collier, S. Weijers, J. Rozema, S. A. Rayback, N. M. Schmidt, G. Schaepman-Strub, S. Wipf, C. Rixen, C. B. Ménard, S. Venn, S. Goetz, L. Andreu-Hayles, S. Elmendorf, V. Ravolainen, J. Welker, P. Grogan, H. E. Epstein, and D. S. Hik. 2011. Shrub expansion in tundra ecosystems: dynamics, impacts and research priorities. Environmental Research Letters **6**:045509.

Nilsen, E. B., and O. Strand. 2017. Populasjonsdynamiske utfordringer knyttet til fragmentering av villreinfjellet. NINA Temahefte **70**:51.

Odland, A. 1996. Differences in the vertical distribution pattern of Betula pubescens in Norway and its ecological significance. Gustav Fischer.
Odland, A., T. Hoitomt, and S. L. Olsen. 2010. Increasing Vascular Plant Richness on 13 High Mountain Summits in Southern Norway since the Early 1970s. Arctic Antarctic and Alpine Research **42**:458-470.
Odland, A., and H. K. Munkejord. 2008. Plants as indicators of snow layer duration in southern Norwegian mountains. Ecological Indicators **8**:57-68.
Odland, A., S. Reinhardt, and A. Pedersen. 2015. Differences in richness of vascular plants, mosses, and liverworts in southern Norwegian alpine vegetation. Plant Ecology & Diversity **8**:37-47.
Odland, A., S. M. Sandvik, D. K. Bjerketvedt, and L. L. Myrvold. 2014. Estimation of lichen biomass with emphasis on reindeer winter pastures at Hardangervidda, S Norway. Rangifer **34**.
Ohmura, A. 1982. Climate and energy balance on the arctic tundra. Journal of Climatology **2**:65-84.
Oke, T. R. 1987. Boundary layer climates. 2nd ed. edition. Routledge, London.
Oksanen, L., and R. Virtanen. 1995. Topographic, altitudinal and regional patterns in continental and suboceanic heath vegetation of northern Fennoscandia. Acta Botanica Fennica **153**:1-80.
Oliphant, A. J., R. A. Spronken-Smith, A. P. Sturman, and I. F. Owens. 2003. Spatial Variability of Surface Radiation Fluxes in Mountainous Terrain. Journal of Applied Meteorology **42**:113-128.
Opedal, Ø. H., W. S. Armbruster, and B. J. Graae. 2015. Linking small-scale topography with microclimate, plant species diversity and intra-specific trait variation in an alpine landscape. Plant Ecology & Diversity **8**:305-315.
Palmqvist, K., & Sundberg, B. (2000). Light use efficiency of dry matter gain in five macro-lichens: relative impact of microclimate conditions and species-specific traits. Plant, Cell & Environment, 23(1), 1-14.
Pearson, R. G., S. J. Phillips, M. M. Loranty, P. S. A. Beck, T. Damoulas, S. J. Knight, and S. J. Goetz. 2013. Shifts in Arctic vegetation and associated feedbacks under climate change. Nature Climate Change **3**:673-677.
Peltoniemi, J. I., Kaasalainen, S., Näränen, J., Rautiainen, M., Stenberg, P., Smolander, H., ... & Voipio, P. (2005). BRDF measurement of understory vegetation in pine forests: dwarf shrubs, lichen, and moss. Remote Sensing of Environment, 94(3), 343-354.
Peltoniemi, J. I., T. Manninen, J. Suomalainen, T. Hakala, E. Puttonen, and A. Riihela. 2010. Land Surface Albedos Computed from BRF Measurements with a Study of Conversion Formulae. Remote Sensing **2**:1918-1940.
Petzold, D. E., and A. N. Rencz. 1975. The Albedo of Selected Subarctic Surfaces. Arctic and Alpine Research **7**:393-398.
Pirazzini, R. 2004. Surface albedo measurements over Antarctic sites in summer. Journal of Geophysical Research: Atmospheres **109**.
Pomeroy, J. W., D. S. Bewley, R. L. H. Essery, N. R. Hedstrom, T. Link, R. J. Granger, J. E. Sicart, C. R. Ellis, and J. R. Janowicz. 2006. Shrub tundra snowmelt. Hydrological Processes **20**:923-941.
Porada, P., A. Ekici, and C. Beer. 2016. Effects of bryophyte and lichen cover on permafrost soil temperature at large scale. Cryosphere **10**:2291-2315.
Press, M. C., J. A. Potter, M. J. W. Burke, T. V. Callaghan, and J. A. Lee. 1998. Responses of a subarctic dwarf shrub heath community to simulated environmental change. Journal of Ecology **86**:315-327.
R Core Team (2019). R: A language and environment for statistical computing. R Foundation for Statistical Computing, Vienna, Austria. Retrieved from https://www.R-project.org/.
Ramanathan, V., R. D. Cess, E. F. Harrison, P. Minnis, B. R. Barkstrom, E. Ahmad, and D. Hartmann. 1989. Cloud-Radiative Forcing and Climate: Results from the Earth Radiation Budget Experiment. Science **243**:57.
Sedlar, J., M. Tjernström, T. Mauritsen, M. D. Shupe, I. M. Brooks, P. O. G. Persson, C. E. Birch, C. Leck, A. Sirevaag, and M. Nicolaus. 2011. A transitioning Arctic surface energy budget: the

impacts of solar zenith angle, surface albedo and cloud radiative forcing. Climate Dynamics **37**:1643-1660.

Shupe, M. D., and J. M. Intrieri. 2004. Cloud Radiative Forcing of the Arctic Surface: The Influence of Cloud Properties, Surface Albedo, and Solar Zenith Angle. Journal of Climate **17**:616-628.

Steinbauer, M. J., J.-A. Grytnes, G. Jurasinski, A. Kulonen, J. Lenoir, H. Pauli, C. Rixen, M. Winkler, M. Bardy-Durchhalter, E. Barni, A. D. Bjorkman, F. T. Breiner, S. Burg, P. Czortek, M. A. Dawes, A. Delimat, S. Dullinger, B. Erschbamer, V. A. Felde, O. Fernández-Arberas, K. F. Fossheim, D. Gómez-García, D. Georges, E. T. Grindrud, S. Haider, S. V. Haugum, H. Henriksen, M. J. Herreros, B. Jaroszewicz, F. Jaroszynska, R. Kanka, J. Kapfer, K. Klanderud, I. Kühn, A. Lamprecht, M. Matteodo, U. M. di Cella, S. Normand, A. Odland, S. L. Olsen, S. Palacio, M. Petey, V. Piscová, B. Sedlakova, K. Steinbauer, V. Stöckli, J.-C. Svenning, G. Teppa, J.-P. Theurillat, P. Vittoz, S. J. Woodin, N. E. Zimmermann, and S. Wipf. 2018. Accelerated increase in plant species richness on mountain summits is linked to warming. Nature **556**:231-234.

Stoy, P. C., L. E. Street, A. V. Johnson, A. Prieto-Blanco, and S. A. Ewing. 2012. Temperature, Heat Flux, and Reflectance of Common Subarctic Mosses and Lichens under Field Conditions: Might Changes to Community Composition Impact Climate-Relevant Surface Fluxes? Arctic, Antarctic, and Alpine Research **44**:500-508.

Sturm, M., T. Douglas, C. Racine, and G. E. Liston. 2005. Changing snow and shrub conditions affect albedo with global implications. Journal of Geophysical Research-Biogeosciences **110**.

Sturm, M., C. Racine, and K. Tape. 2001. Climate change. Increasing shrub abundance in the Arctic. Nature **411**:546-547.

Sundstøl, S. A., and A. Odland. 2017. Responses of Alpine Vascular Plants and Lichens to Soil Temperatures. **54**:17-28.

Swann, A. L., I. Y. Fung, S. Levis, G. B. Bonan, and S. C. Doney. 2010. Changes in Arctic vegetation amplify high-latitude warming through the greenhouse effect. Proc Natl Acad Sci U S A **107**:1295-1300.

Tape, K., M. Sturm, and C. Racine. 2006. The evidence for shrub expansion in Northern Alaska and the Pan-Arctic. Global change biology **12**:686-702.

Théau, J., & Duguay, C. R. (2004). Mapping lichen changes in the summer range of the George River Caribou Herd (Québec-Labrador, Canada) using Landsat imagery (1976-1998). Rangifer, 24(1), 31-50.

Thompson, C., J. Beringer, F. S. Chapin, and A. D. McGuire. 2004. Structural complexity and land-surface energy exchange along a gradient from arctic tundra to boreal forest. Journal of Vegetation Science **15**:397-406.

Tybirk, K., M.-C. Nilsson, A. Michelsen, H. L. Kristensen, A. Shevtsova, M. T. Strandberg, M. Johansson, K. E. Nielsen, T. Riis-Nielsen, B. Strandberg, and I. Johnsen. 2000. Nordic *E. nigrum* Dominated Ecosystems: Function and Susceptibility to Environmental Changes. AMBIO: A Journal of the Human Environment **29**:90-97, 98.

Tømmervik, H., J. W. Bjerke, E. Gaare, B. Johansen, and D. Thannheiser. 2012. Rapid recovery of recently overexploited winter grazing pastures for reindeer in northern Norway. Fungal Ecology **5**:3-15.

Tømmervik, H., B. Johansen, J. A. Riseth, S. R. Karlsen, B. Solberg, and K. A. Høgda. 2009. Above ground biomass changes in the mountain birch forests and mountain heaths of Finnmarksvidda, northern Norway, in the period 1957-2006. Forest Ecology and Management **257**:244-257.

Tømmervik, H., Høgda, K. A., & Solheim, I. (2003). Monitoring vegetation changes in Pasvik (Norway) and Pechenga in Kola Peninsula (Russia) using multitemporal Landsat MSS/TM data. *Remote sensing of Environment*, *85*(3), 370-388.

Vanneste, T., O. Michelsen, B. J. Graae, M. O. Kyrkjeeide, H. Holien, K. Hassel, S. Lindmo, R. E. Kapas, and P. De Frenne. 2017. Impact of climate change on alpine vegetation of mountain summits in Norway. Ecological Research **32**:579-593.

Väisänen, M., Martz, F., Kaarlejärvi, E., Julkunen-Tiitto, R., & Stark, S. (2013). Phenolic responses of mountain crowberry (Empetrum nigrum ssp. hermaphroditum) to global climate change are compound specific and depend on grazing by reindeer (Rangifer tarandus). *Journal of chemical ecology*, *39*(11-12), 1390-1399.

Vavrus, S. J., U. S. Bhatt, and V. A. Alexeev. 2011. Factors Influencing Simulated Changes in Future Arctic Cloudiness. Journal of Climate **24**:4817-4830.

Virtanen, T., and M. Ek. 2014. The fragmented nature of tundra landscape. International Journal of Applied Earth Observation and Geoinformation **27**:4-12.

Vuorinen, K. E. M., L. Oksanen, T. Oksanen, A. Pyykönen, J. Olofsson, and R. Virtanen. 2017. Open tundra persist, but arctic features decline—Vegetation changes in the warming Fennoscandian tundra. Global change biology **23**:3794-3807.

Walker, M. D., C. H. Wahren, R. D. Hollister, G. H. Henry, L. E. Ahlquist, J. M. Alatalo, M. S. Bret-Harte, M. P. Calef, T. V. Callaghan, A. B. Carroll, H. E. Epstein, I. S. Jonsdottir, J. A. Klein, B. Magnusson, U. Molau, S. F. Oberbauer, S. P. Rewa, C. H. Robinson, G. R. Shaver, K. N. Suding, C. C. Thompson, A. Tolvanen, O. Totland, P. L. Turner, C. E. Tweedie, P. J. Webber, and P. A. Wookey. 2006. Plant community responses to experimental warming across the tundra biome. Proc Natl Acad Sci U S A **103**:1342-1346.

Walther, G. R., S. Beissner, and C. A. Burga. 2005. Trends in the upward shift of alpine plants. Journal of Vegetation Science **16**:541-548.

Wickham H (2016). ggplot2: Elegant Graphics for Data Analysis. Springer-Verlag New York. ISBN 978-3-319-24277-4, https://ggplot2.tidyverse.org.

Williamson, S. N., I. C. Barrio, D. S. Hik, and J. A. Gamon. 2016. Phenology and species determine growing-season albedo increase at the altitudinal limit of shrub growth in the sub-Arctic. Glob Chang Biol **22**:3621-3631.

Wilson, S. D., and C. Nilsson. 2009. Arctic alpine vegetation change over 20 years. Global change biology **15**:1676-1684.

Wipf, S., V. Stoeckli, and P. Bebi. 2009. Winter climate change in alpine tundra: plant responses to changes in snow depth and snowmelt timing. Climatic Change **94**:105-121.

Wookey, P. A., R. Aerts, R. D. Bardgett, F. Baptist, K. A. BrÅThen, J. H. C. Cornelissen, L. Gough, I. P. Hartley, D. W. Hopkins, S. Lavorel, and G. R. Shaver. 2009. Ecosystem feedbacks and cascade processes: understanding their role in the responses of Arctic and alpine ecosystems to environmental change. Global change biology **15**:1153-1172.

Xu, L., R. B. Myneni, F. S. Chapin, T. V. Callaghan, J. E. Pinzon, C. J. Tucker, Z. Zhu, J. Bi, P. Ciais, H. Tømmervik, E. S. Euskirchen, B. C. Forbes, S. L. Piao, B. T. Anderson, S. Ganguly, R. R. Nemani, S. J. Goetz, P. S. A. Beck, A. G. Bunn, C. Cao, and J. C. Stroeve. 2013. Temperature and vegetation seasonality diminishment over northern lands. Nature Climate Change **3**:581-586.

Young, K. L., M.-K. Woo, and S. A. Edlund. 1997. Influence of Local Topography, Soils, and Vegetation on Microclimate and Hydrology at a High Arctic Site, Ellesmere Island, Canada. Arctic and Alpine Research **29**:270-284.

7. Tables

Table 1. Sampling regime of all species with six pairs (1 – 6) of measurements. The *F. nivalis* surface was measured during the whole study period paired with one of the other surfaces six times. Numbers of measurements per species are presented with the different aspect categories. Aspect categories are HSM = horizontal surface in morning, NOM = north-facing surface morning, SOM= south-facing surface morning, HSN= horizontal surface at noon, NOA = north-facing surface afternoon, SOA = south-facing surface afternoon, and finally HSA = horizontal surface at afternoon.

Pair of surfaces	Species	Numbers of measurements per aspect							Sum
		HSM	NOM	SOM	HSN	NOA	SOA	HSA	
1	*C. stellaris*	14	15	15	15	15	14	14	102
	F. nivalis	16	16	16	16	16	15	15	110
2	*C. islandica*	8			4			4	12
	F. nivalis	8			4			4	12
3	25 % *E. nigrum*	6			3			3	9
	F. nivalis	6			3			3	9
4	50 % *E. nigrum*	5			3			3	8
	F. nivalis	5			3			3	8
5	75 % *E. nigrum*	6			3			3	9
	F. nivalis	6			3			3	9
6	100 % *E. nigrum*	4			2			2	6
	F. nivalis	4			2			2	6
Sum		86	61	61	45	61	61	45	300

Table 2. Mean and standard deviation (SD), range (min. - max.) of surface albedo for all measurements for the different surfaces, and subsets for the different surfaces for HSMA (horizontal surface in the morning and afternoon), HSN (horizontal surface at noon), NO (north-facing surface), SO (south-facing surface).

Species	Subset of measurements	Number of measurements	Mean ± SD	Range (min. – max.)
C. stellaris	All measurements	102	0.355 ± 0.019	0.312 – 0.391
	HSMA	28	0.364 ± 0.019	0.316 – 0.391
	HSN	15	0.345 ± 0.011	0.325 – 0.365
	NO	30	0.340 ± 0.011	0.312 – 0.355
	SO	29	0.366 ± 0.020	0.320 – 0.390
F. nivalis	All measurements	154	0.343 ± 0.022	0.291 – 0.381
	HSMA	60	0.350 ± 0.022	0.300 – 0.381
	HSN	31	0.325 ± 0.016	0.291 – 0.357
	NO	32	0.332 ± 0.013	0.306 – 0.358
	SO	31	0.357 ± 0.017	0.313 – 0.378
25 % *E. nigrum* cover	All measurements, HSMA + HSN	9	0.292 ± 0.015	0.273 – 0.310
50 % *E. nigrum* cover	All measurements, HSMA + HSN	8	0.230 ± 0.013	0.211 – 0.250
75 % *E. nigrum* cover	All measurements, HSMA + HSN	9	0.180 ± 0.016	0.150 – 0.200
100 % *E. nigrum* cover	All measurements, HSMA + HSN	6	0.150 ± 0.014	0.140 – 0.171
C. islandica	All measurements, HSMA + HSN	12	0.151 ± 0.014	0.131 – 0.173

Table 3. Range (Min. - Max.), and Mean, standard deviation (SD) for cloud factor for all the surfaces, and subsets for the different aspects for HSMA (horizontal surface at morning and afternoon), HSN (horizontal surface at noon), NO (north-facing surface), and SO (south-facing surface).

Species	Subset of measurements	Number of measurements	Range (Min. – Max.)	Mean +- SD
C. stellaris	All measurements	102	0.204 – 0.945	0.361 ± 0.184
	HSMA	28	0.233 – 0.945	0.370 ± 0.191
	HSN	15	0.215 – 0.881	0.390 ± 0.204
	NO	30	0.220 – 0.915	0.355 ± 0.182
	SO	29	0.204 – 0.900	0.344 ± 0.177
F. nivalis	All measurements	154	0.159 – 0.944	0.357 ± 0.173
	HSMA	60	0.224 – 0.944	0.362 ± 0.162
	HSN	31	0.159 – 0.879	0.374 ± 0.194
	NO	32	0.214 – 0.914	0.350 ± 0.200
	SO	31	0.210 – 0.900	0.340 ± 0.170
25 % *E. nigrum* cover	All measurements, HSMA + HSN	9	0.212 – 0.425	0.295 ± 0.067
50 % *E. nigrum* cover	All measurements, HSMA + HSN	8	0.174 – 0.453	0.320 ± 0.089
75 % *E. nigrum* cover	All measurements, HSMA + HSN	9	0.245 – 0.540	0.380 ± 0.110
100 % *E. nigrum* cover	All measurements, HSMA + HSN	6	0.240 – 0.800	0.460 ± 0.230

C. islandica	All measurements, HSMA + HSN	12	0.131 – 0.173	0.15 ± 0.014

8. Figures

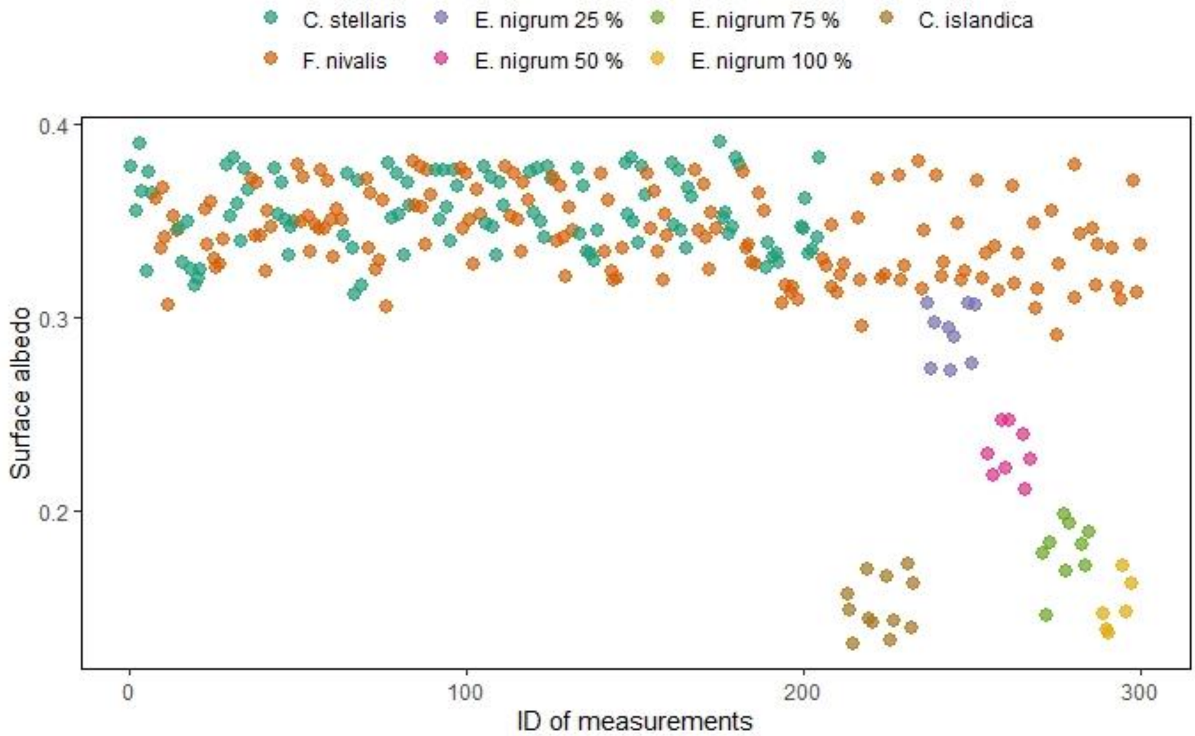

Figure 1. Surface albedo measurements of all species *C. stellaris* (turquoise), *F. nivalis* (orange), *E. nigrum* 25 % (purple), *E. nigrum* 50 % (pink), *E. nigrum* 75 % (green), *E. nigrum* 100 % (yellow), and *C. islandica* (brown) with ID of the (n=300) measurements.

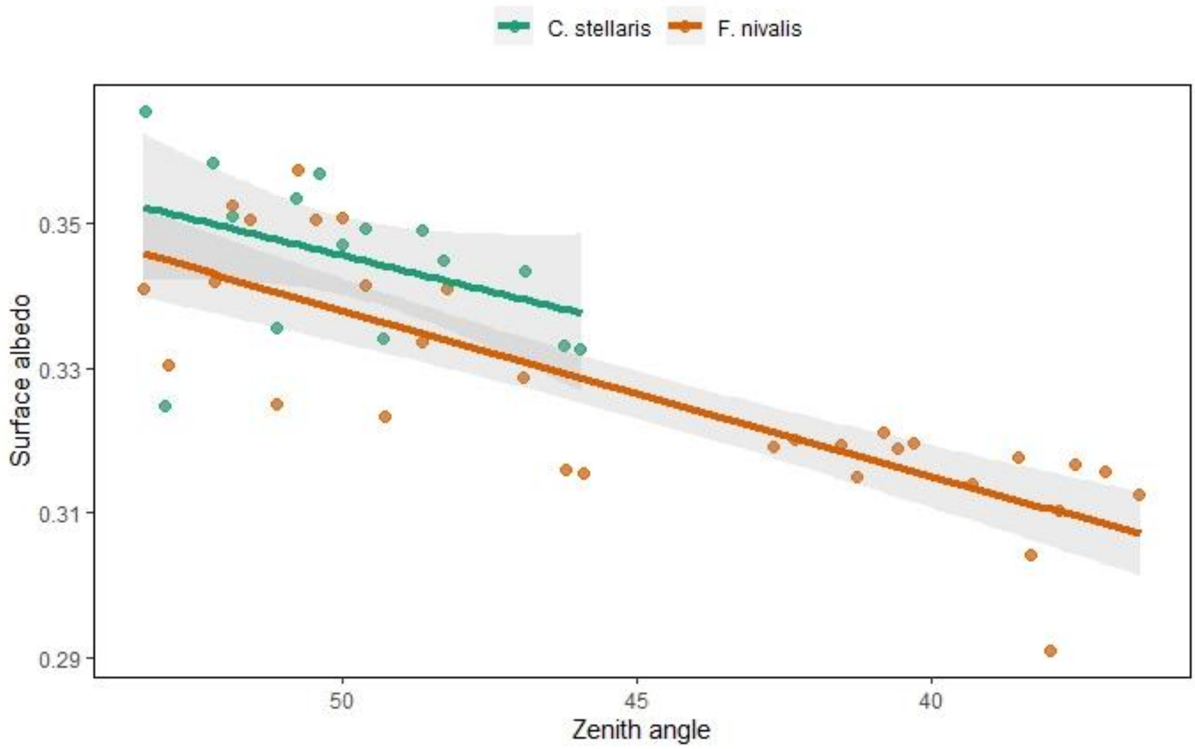

Figure 2. Relation between surface albedo and zenith angle for *C. stellaris* (turquoise) and *F. nivalis* (orange) with 95 % confidence interval.

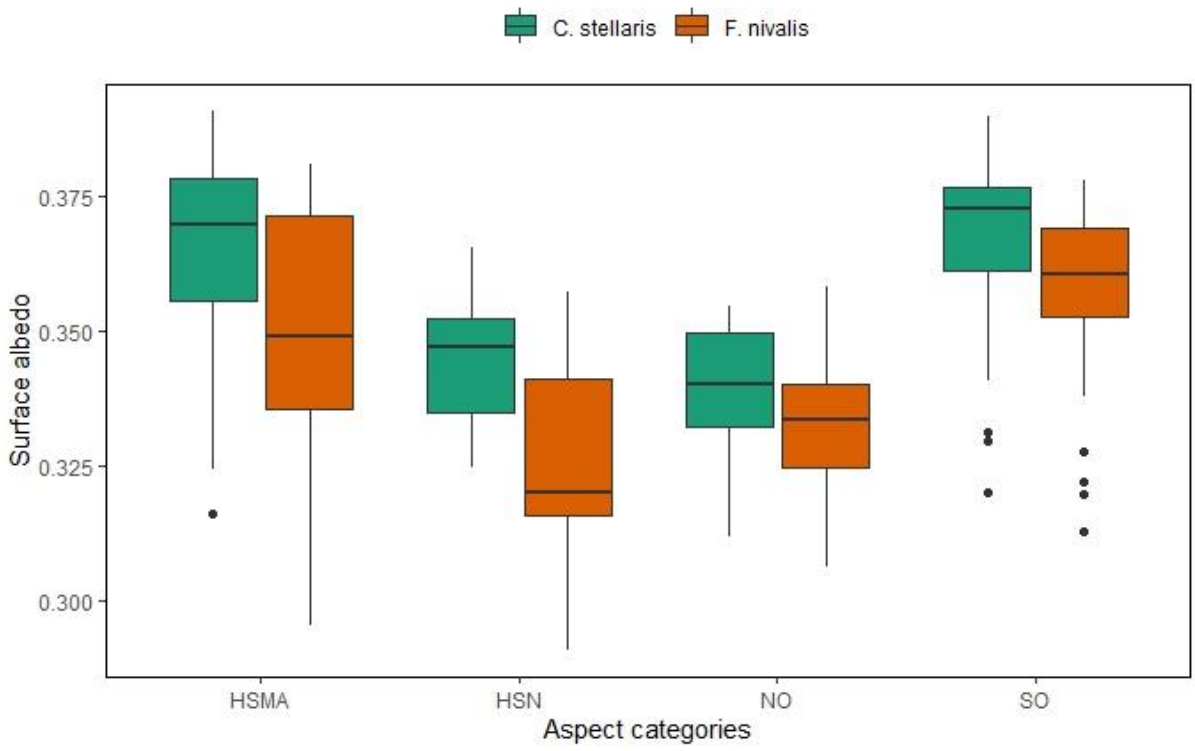

Figure 3. Relation between surface albedo and aspect. Aspect categories are horizontal surface at morning and afternoon (HSMA), horizontal surface at noon (HSN), north-facing surface (NO), and south-facing surface (SO) for *C. stellaris* (turquoise) and *F. nivalis* (orange).

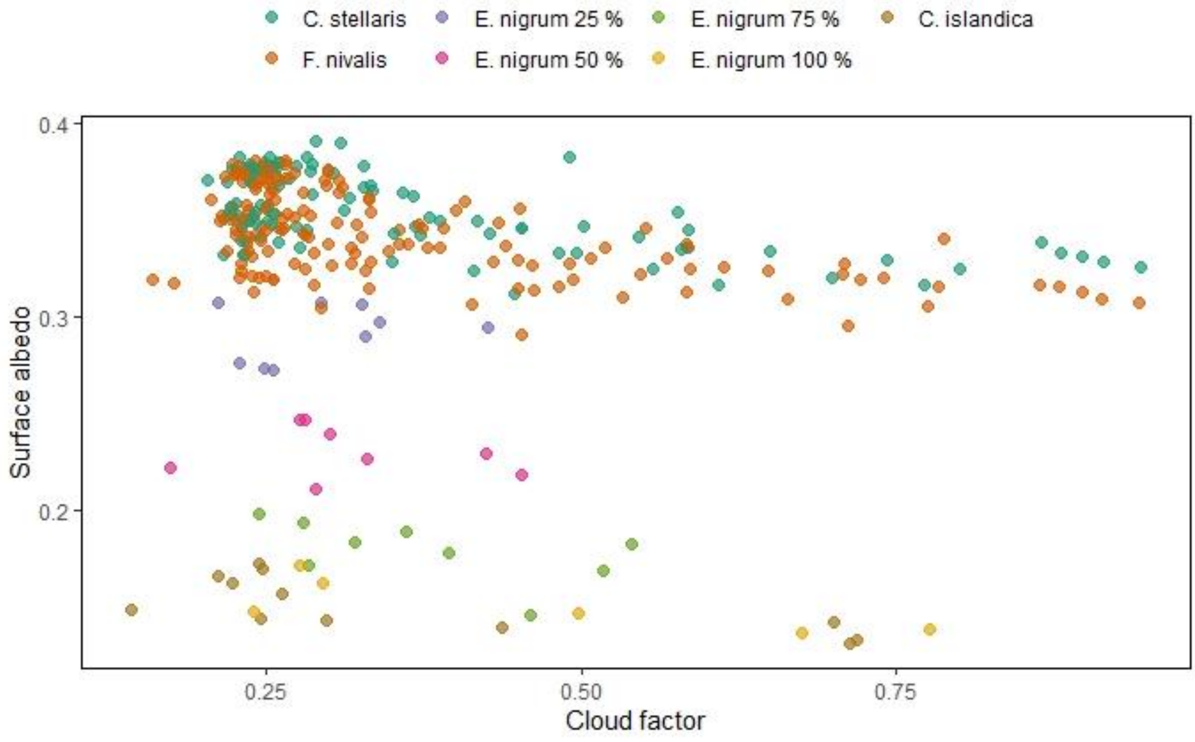

Figure 4. Relation between surface albedo and cloud factor for all species *C. stellaris* (turquoise), *F. nivalis* (orange), *E. nigrum* 25 % (purple), *E. nigrum* 50 % (pink), *E. nigrum* 75 % (green), *E. nigrum* 100 % (yellow), and *C. islandica* (brown).

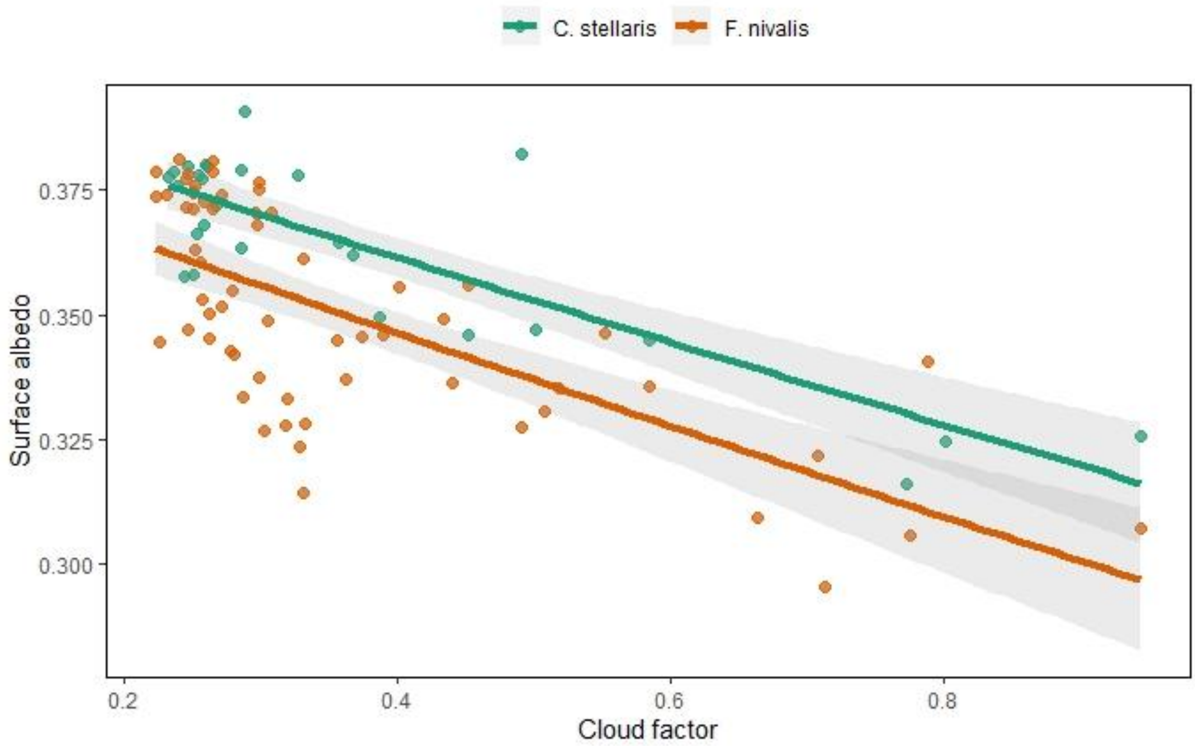

Figure 5. Relation between surface albedo and cloud factor for *C. stellaris* (turquoise) and *F. nivalis* (orange) with 95 % confidence interval.

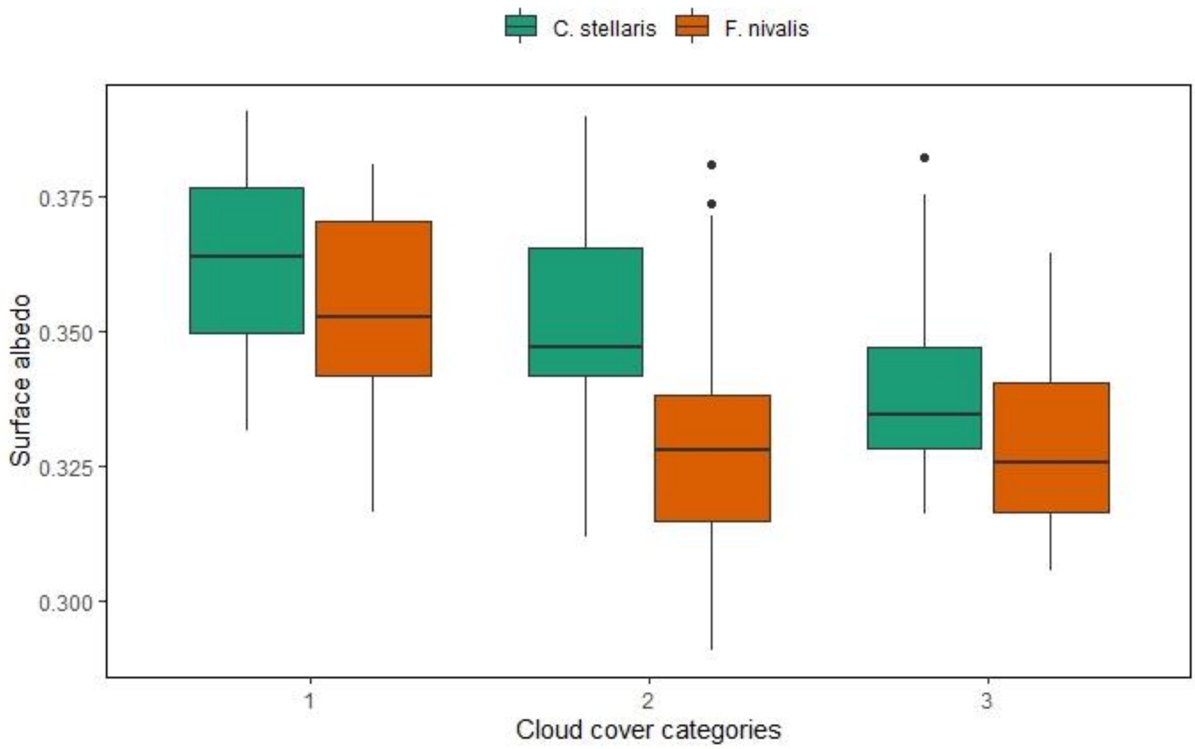

Figure 6. Surface albedo and cloud cover observations for all measurements on *C. stellaris* (turquoise) and *F. nivalis* (orange) for three cloud cover categories.

9. Appendix

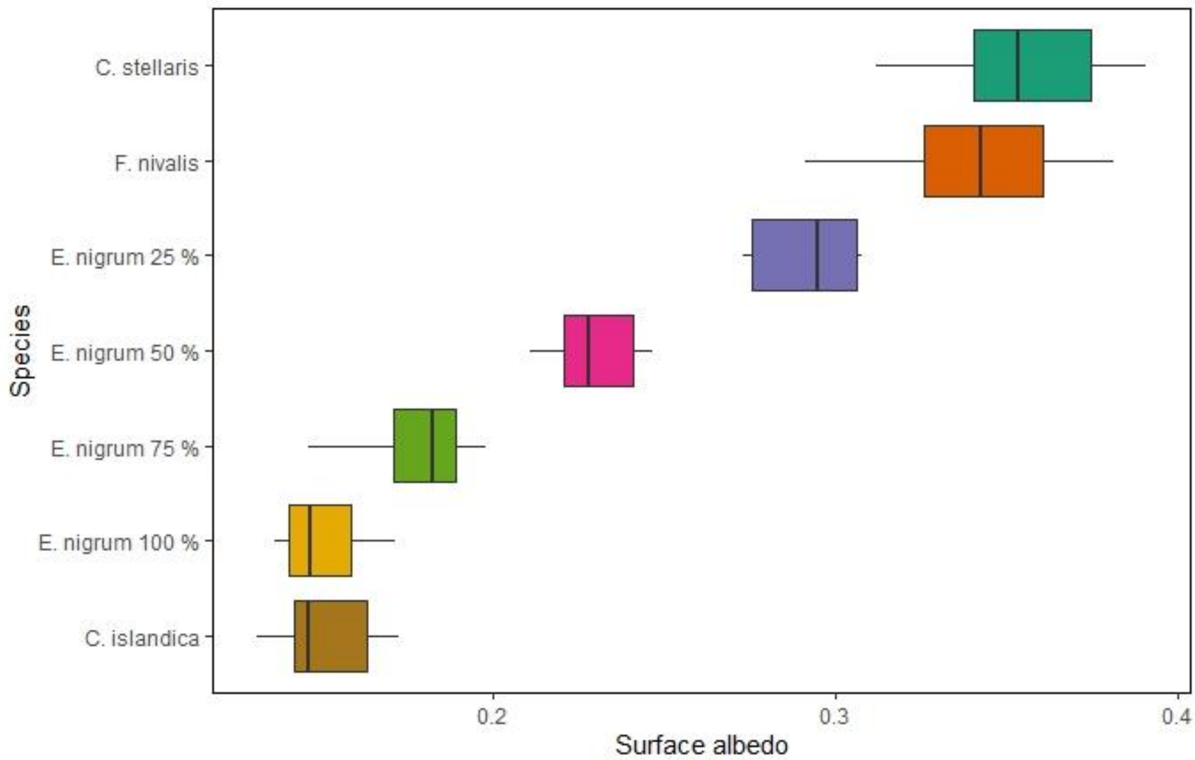

Figure A2. Surface albedo of all species *C. stellaris* (turquoise), *F. nivalis* (orange), *E. nigrum* 25 % (purple), *E. nigrum* 50 % (pink), *E. nigrum* 75 % (green), *E. nigrum* 100 % (yellow), and *C. islandica* (brown) measurements. Axes are reversed.

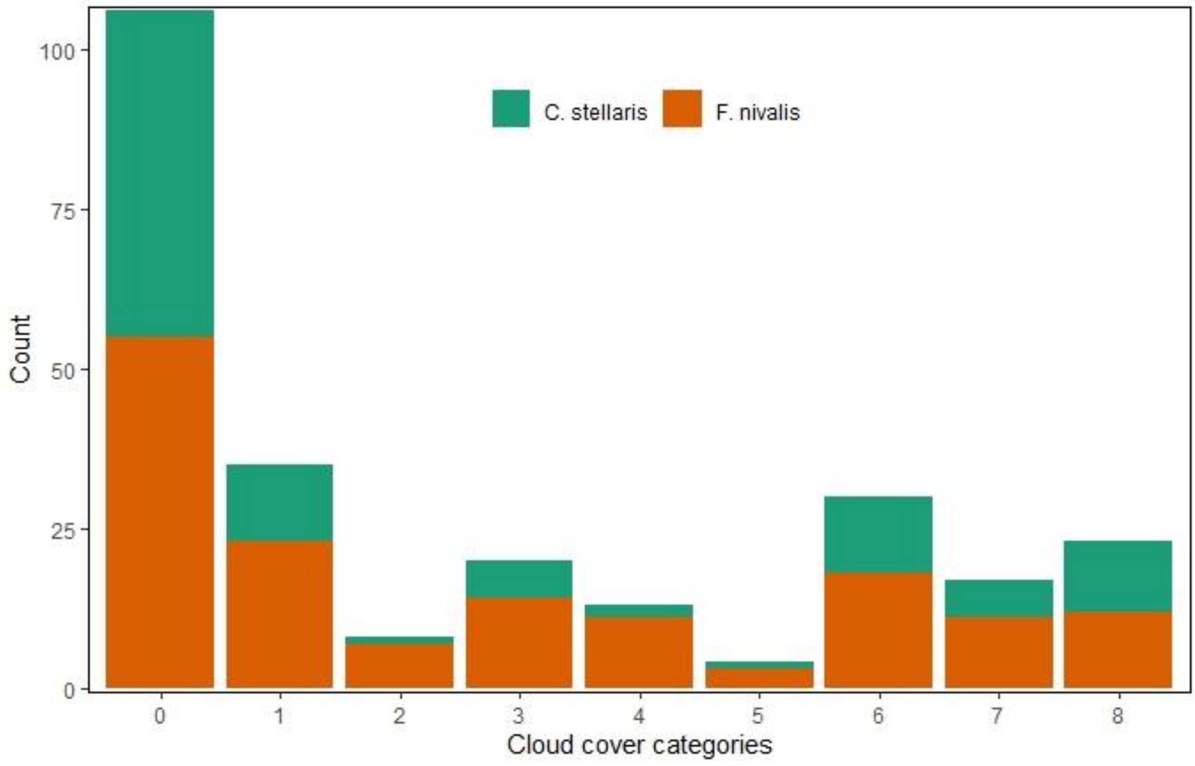

Figure A2. Counts of cloud cover categories per species of *C. stellaris* (turquoise) and *F. nivalis* (orange) from the 9 cloud cover categories ranging from 0 to 8 in okta units.

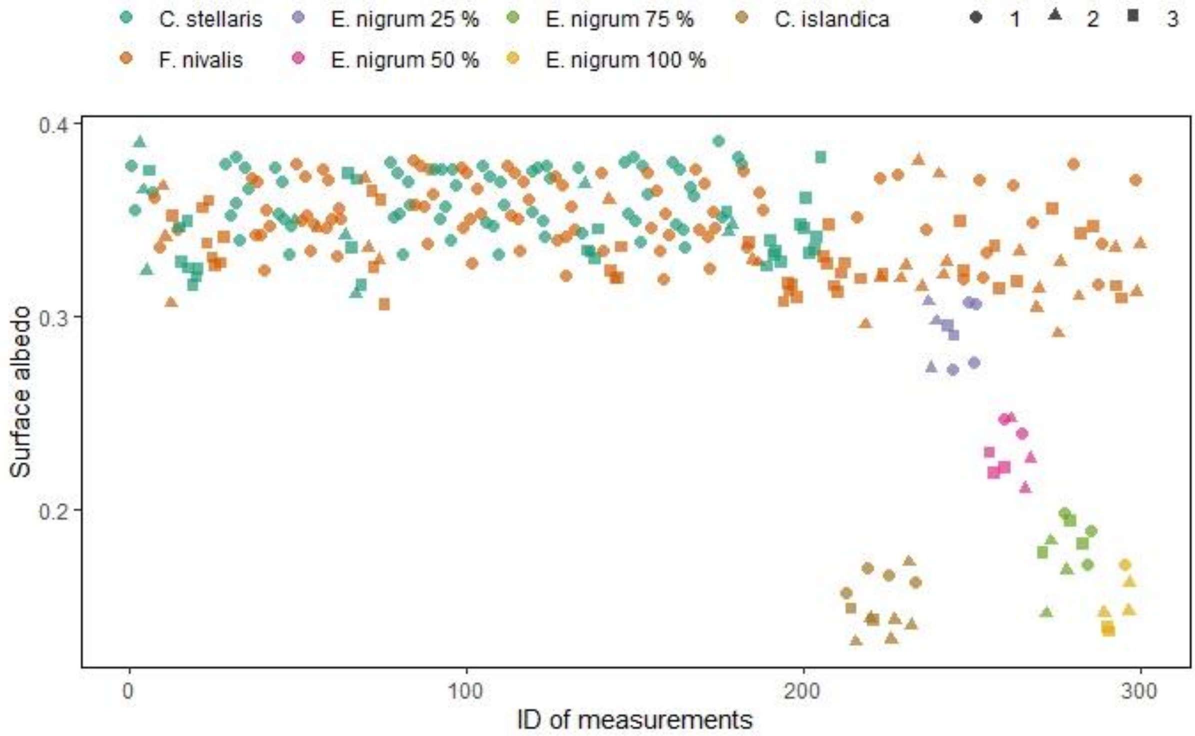

Figure A3. Surface albedo of all species of *C. stellaris* (turquoise), *F. nivalis* (orange), *E. nigrum* 25 % (purple), *E. nigrum* 50 % (pink), *E. nigrum* 75 % (green), *E. nigrum* 100 % (yellow), and *C. islandica* (brown) with cloud cover group 1 (circle), 2 (triangle) and 3 (square).

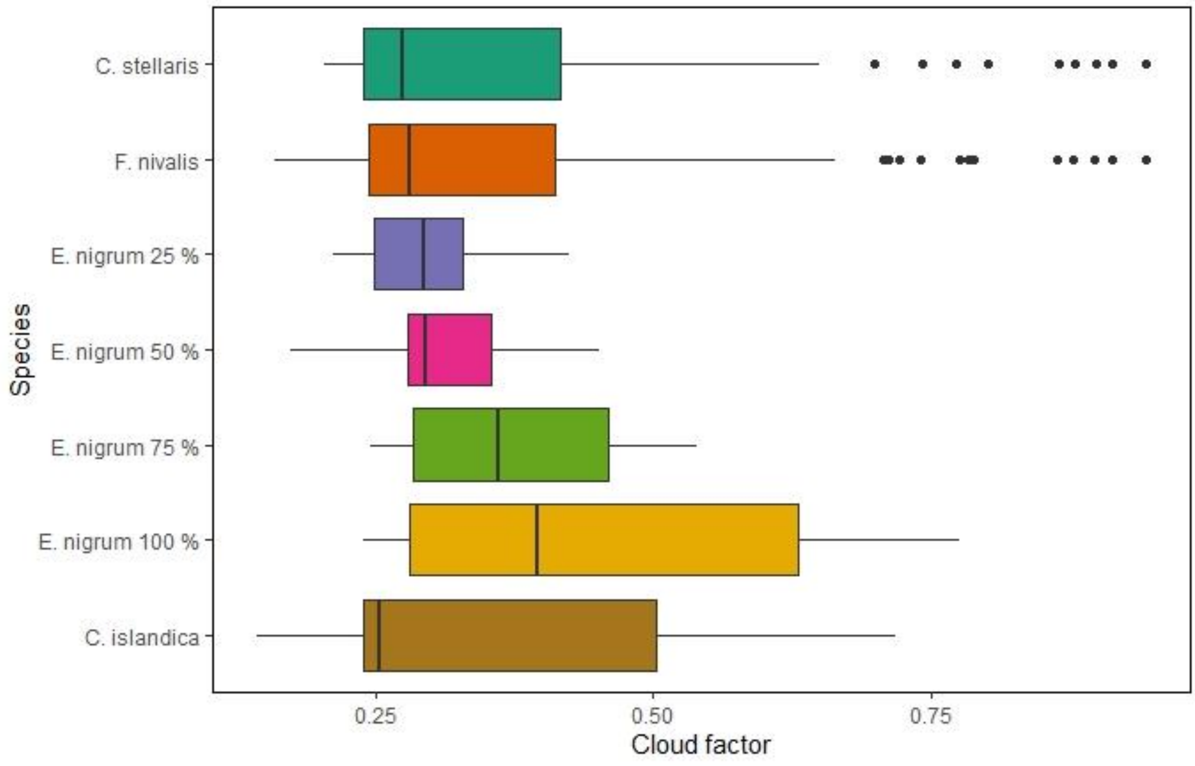

Figure A4. Cloud factor for all species *C. stellaris* (turquoise), *F. nivalis* (orange), *E. nigrum* 25 % (purple), *E. nigrum* 50 % (pink), *E. nigrum* 75 % (green), *E. nigrum* 100 % (yellow), and *C. islandica* (brown) measurements. Axis are reversed.

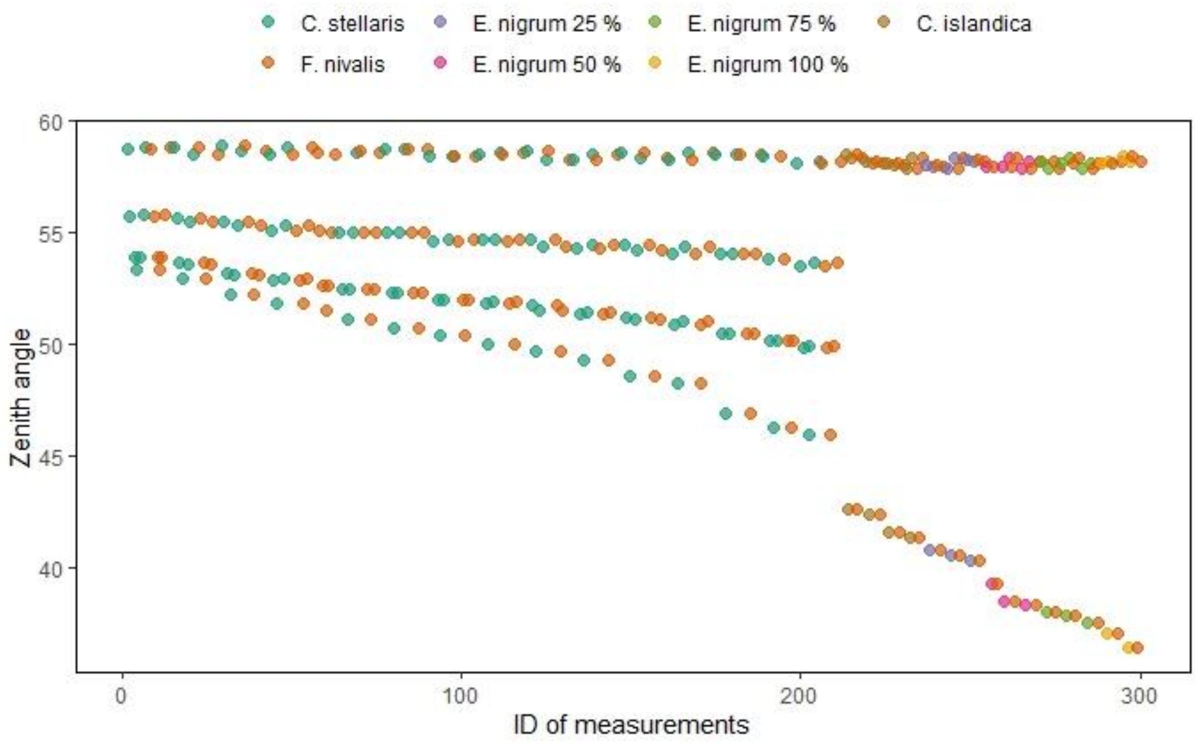

Figure A5. Zenith angles for surface albedo measurements through the whole study period for all species. The graph show that measurements are paired. The data points positioned lower in the figure show decreasing zenith angle from April to June.

Table A1. Counts of cloud cover observations per species of *C. stellaris* and *F. nivalis* for the different cloud cover categories ranging from 0 to 8 in okta units.

Counts per species	Okta units								
	0	1	2	3	4	5	6	7	8
C. stellaris	51	12	1	6	2	1	12	6	11
F. nivalis	55	23	7	14	11	3	18	11	12

Table A2. Mean and standard deviation (SD), and range (min. - max.) for the surface albedo of all measurements under different cloud cover categories for *C. stellaris* and *F. nivalis*. Subsets are displayed for the different species for HSMA (horizontal surface at morning and afternoon), HSN (horizontal surface at noon), for cloud cover category of 0 cloud cover, and regrouping of cloud cover to category 1, 2 and 3.

Species	Subset of measurements	Number of measurements	Mean ± SD	Range (min. – max.)
C. stellaris	0 cloud cover	51	0.363 ± 0.015	0.332 – 0.391
	0 cloud cover, HSMA	17	0.373 ± 0.009	0.360 – 0.391
	0 cloud cover, HSMA + HSN	24	0.370 ± 0.012	0.350 – 0.391
	1 cloud cover	64	0.362 ± 0.020	0.332 – 0.391
	2 cloud cover	9	0.349 ± 0.023	0.312 – 0.390
	3 cloud cover	29	0.341 ± 0.020	0.316 – 0.382
	1 cloud cover, HSMA	20	0.373 ± 0.010	0.360 – 0.391
	2 cloud cover, HSMA	1	0.350 ± 0	
	3 cloud cover, HSMA	7	0.341 ± 0.022	0.316 – 0.382
F. nivalis	0 cloud cover	55	0.360 ± 0.020	0.320 – 0.381
	0 cloud cover, HSMA	21	0.363 ± 0.014	0.333 – 0.381
	0 cloud cover, HSMA + HSN	28	0.360 ± 0.014	0.333 – 0.381

	1 cloud cover	85	0.354 ± 0.017	0.320 – 0.381
	2 cloud cover	28	0.331 ± 0.023	0.291 – 0.381
	3 cloud cover	41	0.330 ± 0.016	0.310 – 0.364
	1 cloud cover, HSMA	33	0.362 ± 0.014	0.333 – 0.381
	2 cloud cover, HSMA	12	0.339 ± 0.025	0.300 – 0.381
	3 cloud cover, HSMA	15	0.333 ± 0.017	0.310 – 0.356

Table A3. Model average results from the top model set (Δ AICc<2) predicting environmental factors influence on the surface albedo. Model terms estimate are presented on a log scale, standard error (SE), t value, Pr(>|z|), confidence intervals (CI) and under-dispersion are reported. All informative model terms (CI do not include 0) are marked with an asterisk.

Response variable	Predictor	Estimate	SE	t value	Pr(>|z|)	CI upper	CI lower	Under-dispersion
Surface albedo	Intercept	-0.981	0.014	-68.915	< 2e-16	-1.009	-0.953*	0.006
	E. nigrum 100%	-0.816	0.011	-73.432	< 2e-16	-0.838	-0.794*	
	E. nigrum 25 %	-0.175	0.009	-18.978	< 2e-16	-0.194	-0.157*	
	E. nigrum 50 %	-0.392	0.010	-40.043	< 2e-16	-0.412	-0.373*	
	E. nigrum 75 %	-0.654	0.009	-70.970	< 2e-16	-0.672	-0.636*	
	F. nivalis	-0.027	0.003	-9.855	< 2e-16	-0.032	-0.021*	
	C. islandica	-0.835	0.008	-103.187	< 2e-16	-0.851	-0.819*	
	Cloud factor	-0.192	0.026	-7.382	1.56e-13	-0.243	-0.141*	
	Aspect HSN	0.005	0.021	0.234	0.815*	-0.037	0.047	
	Aspect NO	-0.031	0.014	-2.242	0.025	-0.058	-0.004*	
	Aspect SO	0.040	0.014	2.967	0.003	0.014	0.067*	
	Zenith	0.032	0.008	4.003	6.24e-05	0.016	0.048*	

Table A4. Model selection for generalized linear mixed model from a global set of models. Model terms included in each model are displayed with estimates and AICc, Δ AICc and Akaike weight. Only model with Δ AICc<2 are used in the top model.

Response variable	Intercept	Aspect	Cloud factor	Species	Zenith	df	logLik	AICc	Delta AICc	Weight
Surface albedo	-0.981	+	-0.192	+	0.032	15	1008.929	-1986.168	0.000	9.977e-01
	-0.948	+	-0.210	+		14	1001.751	-1974.029	12.139	2.307e-03
	-0.978		-0.188	+	0.031	12	993.267	-1961.448	24.720	4.276e-06
	-1.054	+		+	0.034	14	987.062	-1944.651	41.518	9.627e-10

Table A5. Sampling regime of all measurements. Aspect categories HSM = horizontal surface in morning, NOM = north-facing surface morning, SOM= south-facing surface morning, HSN= horizontal surface at noon, NOA = north-facing surface afternoon, SOA = south-facing surface afternoon, and finally HSA = horizontal surface at afternoon, zenith angles and cloud cover categories are presented. Date for each measurement and each species. Cloud cover is presented in okta units, from 0 to 8. Comments on species that are not measured.

Aspect	HSM	NOM	SOM	HSN	NOA	SOA	HSA		
Zenith angle	58	55	53	53-36	53	55	58		
Date	Cloud cover							Species	Comments
05.04.2019	0	0	3	3	3	6	0	Cl + Fl	
06.04.2019	8	6	6	7	8	7	8	Cl + Fl	
08.04.2019	0	0	0	0	0	0	0	Cl + Fl	
09.04.2019	0	0	0	0	1	2	3	Cl + Fl	
10.04.2019	1	1	1	1	1	1	2	Fl	Cl not measured
11.04.2019	3	4	6	6	5	6	6	Cl + Fl	Cl not measured HSM
12.04.2019	0	0	0	0	0	0	0	Cl + Fl	
13.04.2019	0	0	0	0	0	0	0	Cl + Fl	
14.04.2019	0	0	0	0	0	0	0	Cl + Fl	
15.04.2019	0	0	0	0	0	0	0	Cl + Fl	
16.04.2019	1	1	3	7	7	7	6	Cl + Fl	
18.04.2019	0	0	0	0	0	0	0	Cl + Fl	
19.04.2019	1	1	1	1	1	1	1	Cl + Fl	
23.04.2019	0	1	6	4	3	1	0	Cl + Fl	
25.04.2019	8	8	8	8	8			Cl + Fl	Both species not measured SOA+HSA
26.04.2019	8	8	7	6	8	6	6	Cl + Fl	
08.05.2019	2			5			6	Fl + Is	
11.05.2019	0			4			3	Fl + Is	
12.05.2019	3			3			1	Fl + Is	

13.05.2019	4			4			1	Fl + Is	
14.05.2019	4			3			4	25 + Fl	
15.05.2019	7			1			6	25 + Fl	
16.05.2019	0			2			0	25 + Fl	
21.05.2019	7			8				50 + Fl	Both species not measured HSA
25.05.2019	0			7			4	50 + Fl	
26.05.2019	2			3			4	50 + Fl	
28.05.2019	6			4			3	75 + Fl	
29.05.2019	1			4			6	75 + Fl	
31.05.2019	7			1			1	75 + Fl	
04.06.2019	3			6			7	100 + Fl	
10.06.2019	2			4			4	100 + Fl	

HSN